Simultaneous alleviation of major cosmological tensions through Λ_sCDM cosmology

Özgür Akarsu
Istanbul Technical University

Based on the works in collaboration with John D. Barrow, Eleonora Di Valentino, Luis A. Escamilla, Suresh Kumar, Rafael Nunes, Emre Özülker, J. Alberto Vazquez, Anita Yadav

Workshop on Tensions in Cosmology
6 September-12 September 2023
Corfu, Greece

İTÜ 250 YIL 1773–2023

TÜRKİYE BİLİMLER AKADEMİSİ
TURKISH ACADEMY OF SCIENCES

TÜBİTAK

ANOMALIES & TENSIONS IN COSMOLOGY • COSMOVERSE •

cost
EUROPEAN COOPERATION
IN SCIENCE & TECHNOLOGY

Graduated dark energy: observational hints of a spontaneous sign switch in the cosmological constant

Akarsu, Barrow, Escamilla & Vazquez, PRD (2020), arXiv:1912.08751

$$\nabla_\mu G^{\mu\nu} = 0 \xrightarrow[G_{\mu\nu} = -T_{\mu\nu}]{\text{GR}} \nabla_\mu T^{\mu\nu} = 0$$

$\dot{\rho} + \Theta\varrho = 0$ (Local energy conservation)

$\mathrm{D}^\mu p + \varrho \dot{u}^\mu = 0$ (Newton's 2nd law of motion)

$\varrho = \rho + p$ (Inertial mass density)

Cosmological Constant or the usual vacuum energy of QFT

$$\varrho_\Lambda = 0$$

See Nihan's talk

Simple-gDE:

$$\varrho = \text{constant}$$

Acquaviva, Akarsu, Katırcı & Vazquez PRD (2021), arXiv:2104.02623

gDE: Graduated dark energy

$$\varrho = \gamma\rho_0 \left(\frac{\rho}{\rho_0}\right)^\lambda$$

The simplest dynamical deviation from zero inertial mass density of the usual vacuum energy density. Inspired by *Graduated inflationary universes*, Barrow, PLB, 1990.

$$\rho = \rho_0 \left[1 + 3\gamma(\lambda - 1)\ln a\right]^{\frac{1}{1-\lambda}} \xrightarrow{\frac{1}{1-\lambda} = \frac{m}{n}} \rho = \rho_0\, \mathrm{sgn}[1 - \Psi \ln a]\, |1 - \Psi \ln a|^{\frac{1}{1-\lambda}}$$

m and *n* are odd integers

EoS parameter

$$w = -1 + \frac{\gamma}{1 + 3\gamma(\lambda - 1)\ln a}$$

$$\Psi \equiv -3\gamma(\lambda - 1) < 0 \qquad \lambda < 1 \qquad \gamma < 0$$

Sign changing energy density requires an EoS exhibiting a singularity/pole. (Özülker, PRD 2022, arXiv:2203.04167)

See Emre's talk

Under these conditions energy density takes negative values in the past and EoS exhibits singularity/pole during its sign change

gDE-CDM, replaces the Λ of ΛCDM with the gDE

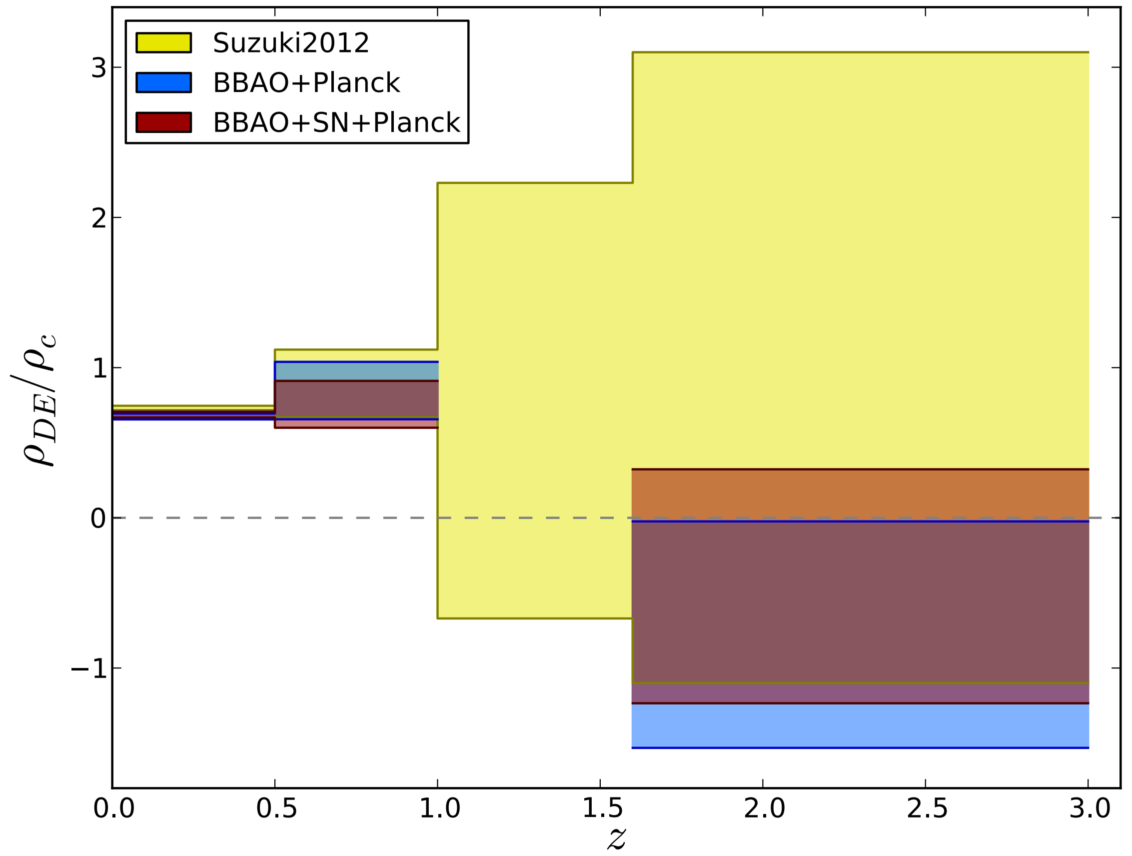

Aubourg et al. (BOSS Collab.), PRD (2015), arXiv:1411.1074

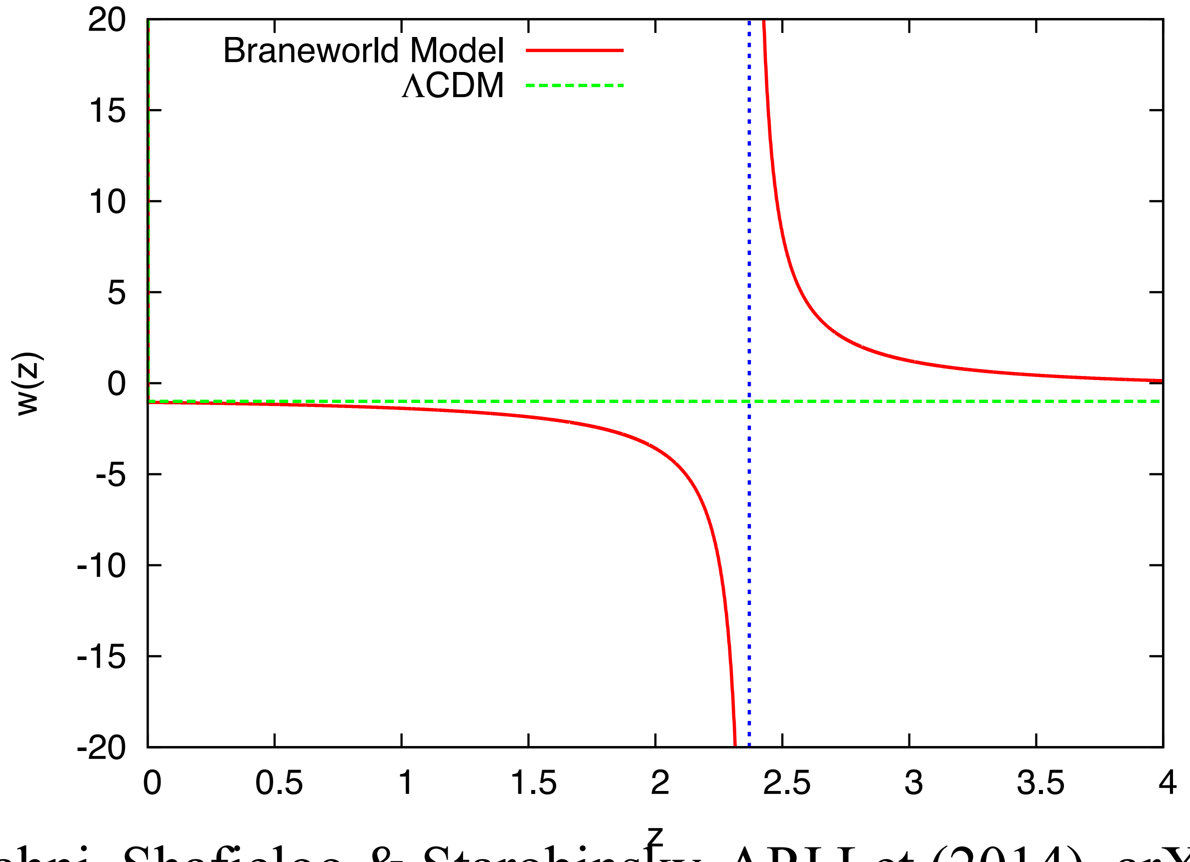

Sahni, Shafieloo & Starobinsky, APJ Let (2014), arXiv:1406.2209

$$\frac{H^2}{H_0^2} = \Omega_{\rm r,0}a^{-4} + \Omega_{\rm m,0}a^{-3} + \Omega_{\rm DE,0}\,{\rm sgn}[1-\Psi\ln a]\,|1-\Psi\ln a|^{\frac{1}{1-\lambda}}$$

$$\frac{\rho_{\rm DE}}{\rho_{\rm c,0}} = \Omega_{\rm DE,0}\,{\rm sgn}[1-\Psi\ln a]\,|1-\Psi\ln a|^{\frac{1}{1-\lambda}}$$

$$\rho_{\rm gDE} = \rho_{\rm gDE0}\,{\rm sgn}[1+\Psi\ln(1+z)]\,|1+\Psi\ln(1+z)|^{\frac{1}{1-\lambda}}$$

gDE density changes sign at $z_\dagger = {\rm e}^{-\Psi^{-1}} - 1$

Λ_sCDM?

$$\frac{\rho_{\rm DE}}{\rho_{\rm c,0}} \to \Omega_{\rm DE,0}\,{\rm sgn}[1-\Psi\ln a] \quad \text{as} \quad \lambda\to-\infty$$

$$\Lambda \quad \to \quad \Lambda_{\rm s} \equiv \Lambda_{\rm s0}\,{\rm sgn}[z_\dagger - z]$$

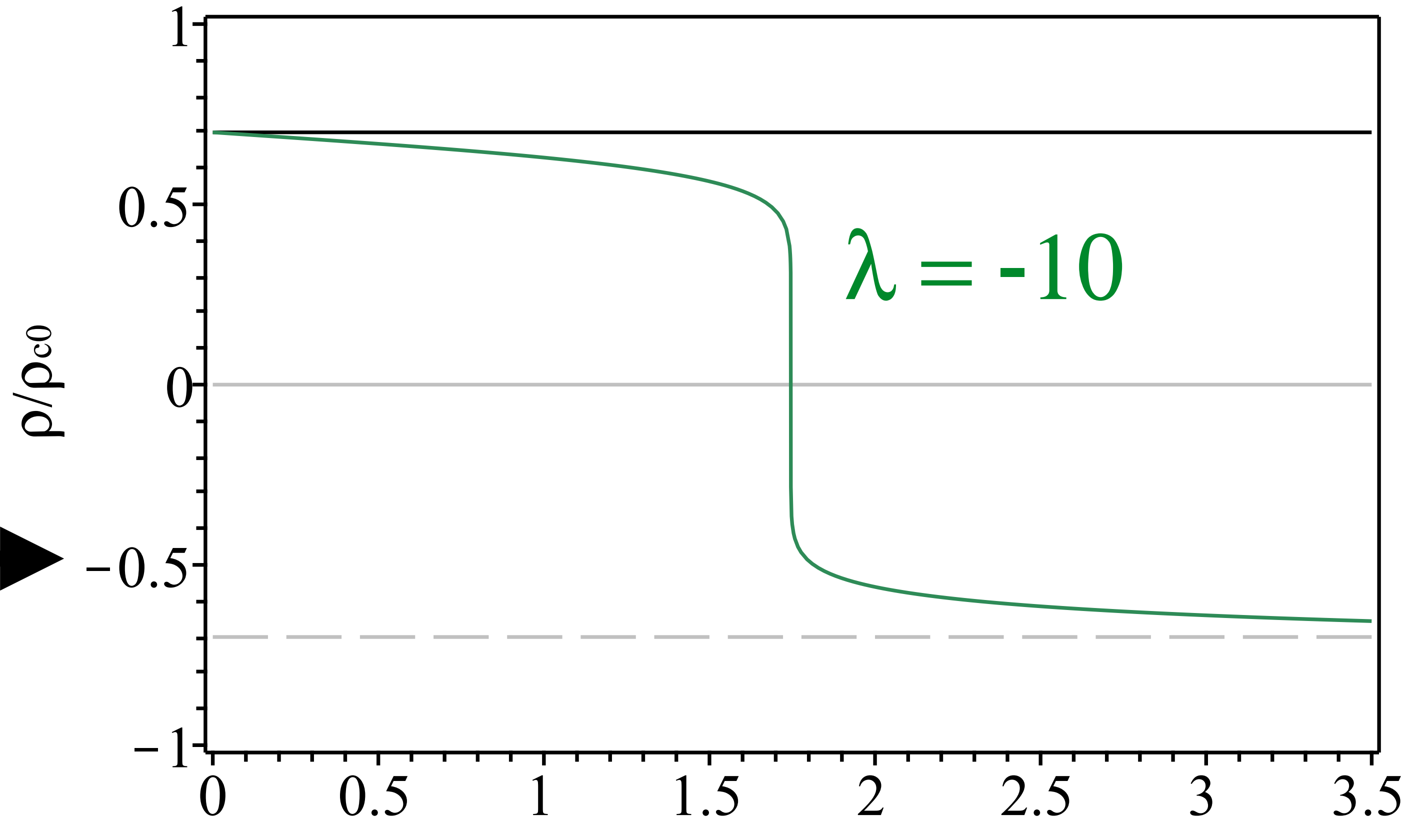

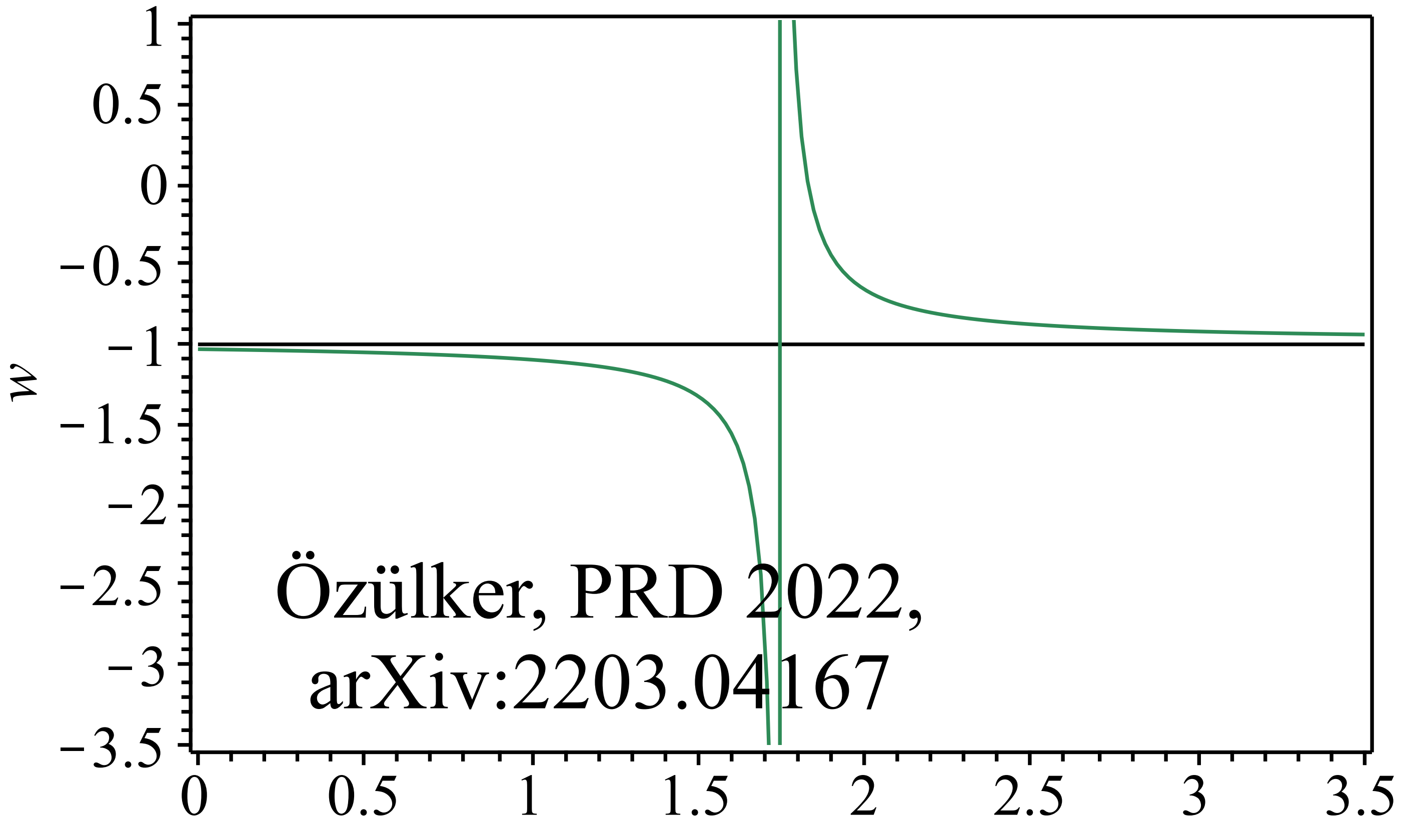

Özülker, PRD 2022, arXiv:2203.04167

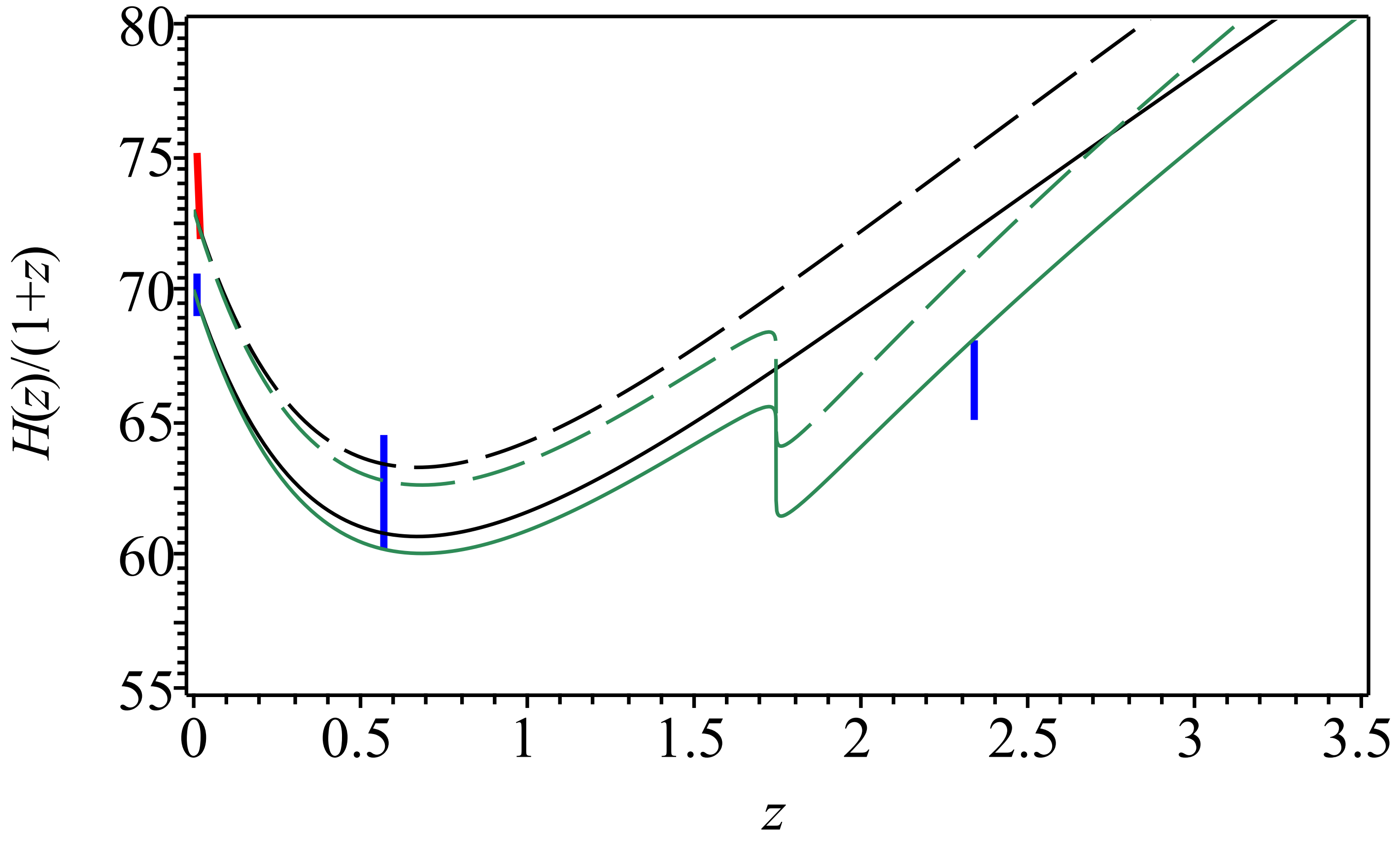

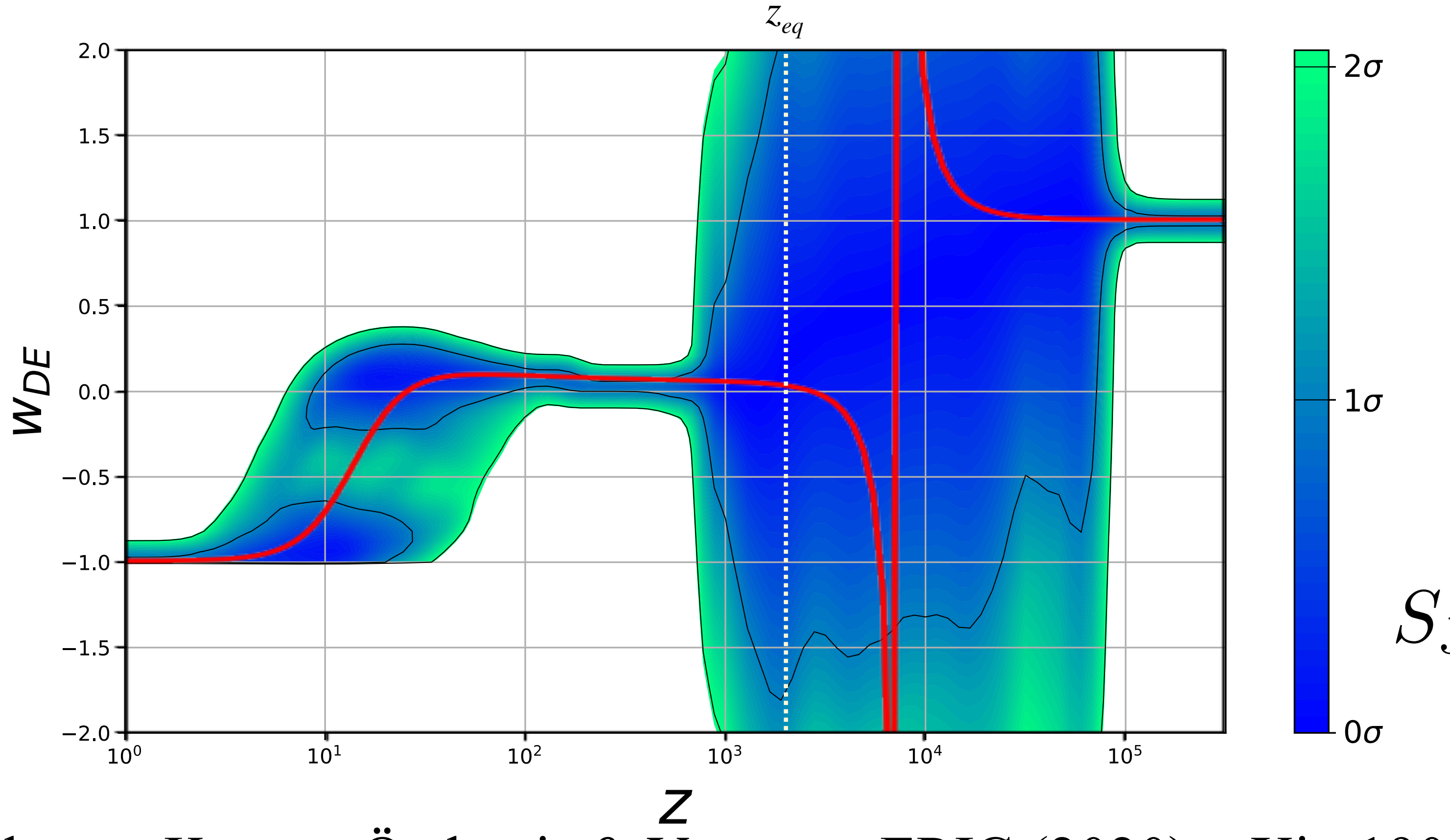

Akarsu, Katırcı, Özdemir & Vazquez, EPJC (2020) arXiv:1903.06679

Massive Brans-Dicke gravity extension of the standard ΛCDM model

$$S_{\rm JBD} = \int {\rm d}^4x\sqrt{-g}\left[\frac{\varphi^2}{8}R - \omega\left(\frac{1}{2}\nabla_\mu\varphi\nabla^\mu\varphi + \frac{1}{2}M^2\varphi^2\right)\right] + S_{\rm Matter},$$

Constraints on gDE-CDM from PLK+BAO+SN (JLA)+H (Cosmic Chronometers)

	λ	$\Omega_{m,0}$	h_0	$\gamma = w_0 + 1$	Ψ	z_*	t_0[Gyr]	$-2\Delta \ln \mathcal{L}_{max}$
	ΛCDM	0.302(6)	0.682(5)	0	0	–	13.806(22)	0.0
	0	0.297(7)	0.689(7)	> -0.08	> -0.25	–	13.796(24)	0.02
	−2	0.297(7)	0.688(7)	> -0.06	> -0.61	–	13.795(25)	0.02
	−4	0.289(6), 0.298(7)	0.700(9), 0.686(7)	−0.057(2), > -0.048	−0.86(3), > -0.73	2.31(12),–	13.714(25), 13.791(26)	1.0, 0.02
	−6	0.292(6), 0.299(6)	0.699(9), 0.685(7)	−0.039(1), > -0.037	−0.86(3), > -0.77	2.31(12),–	13.715(25), 13.792(27)	2.0, 0.01
	−10	0.294(6), 0.299(6)	0.696(8), 0.684(7)	−0.025(1), > -0.021	−0.86(3), > -0.69	2.32(12),–	13.722(27), 13.797(25)	4.4, 0.02
	−14	0.296(6), 0.300(6)	0.695(8), 0.683(7)	−0.019(1), > -0.017	−0.86(3), > -0.76	2.33(12),–	13.719(31), 13.794(27)	5.3, 0.01
	−20	0.297(6), 0.300(6)	0.696(9), 0.683(7)	−0.013(1), > -0.012	−0.86(3), > -0.76	2.32(12),–	13.718(31), 13.795(26)	6.0, 0.02
λ free	−17.9(5.8)	0.296(6), 0.299(7)	0.697(9), 0.684(8)	−0.017(8), > -0.074	−0.85(4), > -0.69	2.32(19),–	13.719(30), 13.795(24)	6.4, 0.01

New max. **Old max.**

$$z_{\dagger} = e^{-\Psi^{-1}} - 1$$

$$\Psi \equiv -3\gamma(\lambda - 1) < 0$$

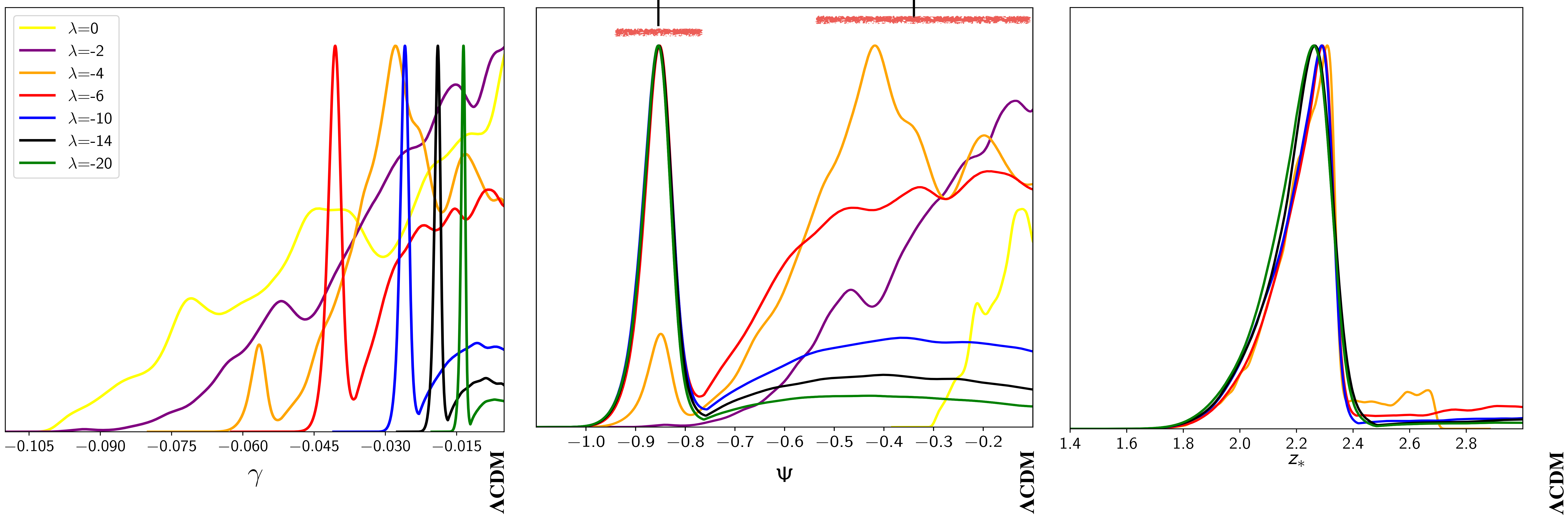

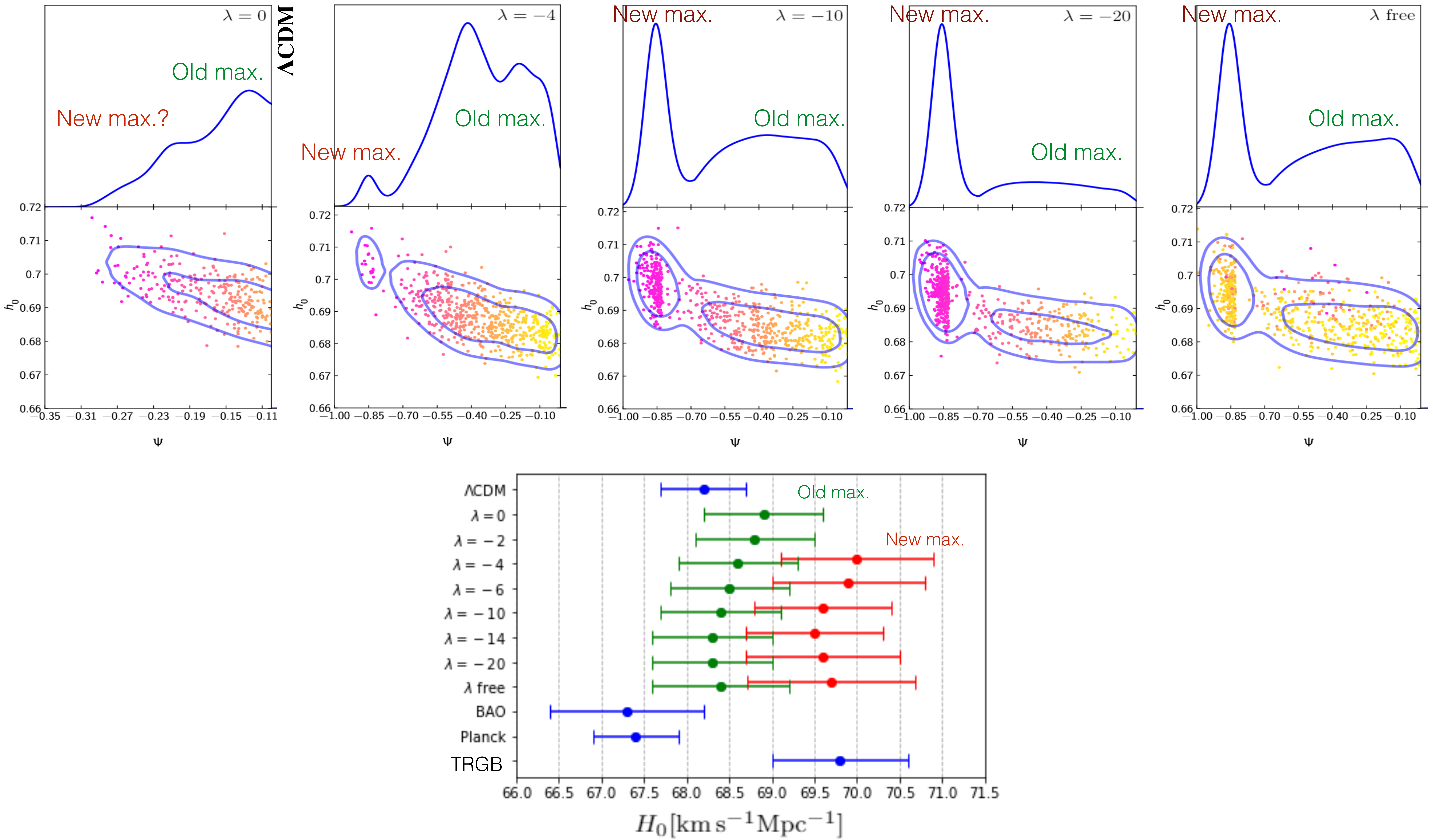

λ = 0
Old max.
New max.?
ΛCDM
λ = −4
Old max.
New max.
New max.
λ = −10
Old max.
New max.
λ = −20
Old max.
New max.
λ free
Old max.
h0
Ψ
ΛCDM
λ = 0
λ = −2
λ = −4
λ = −6
λ = −10
λ = −14
λ = −20
λ free
BAO
Planck
TRGB
Old max.
New max.
H0 [km s−1 Mpc−1]

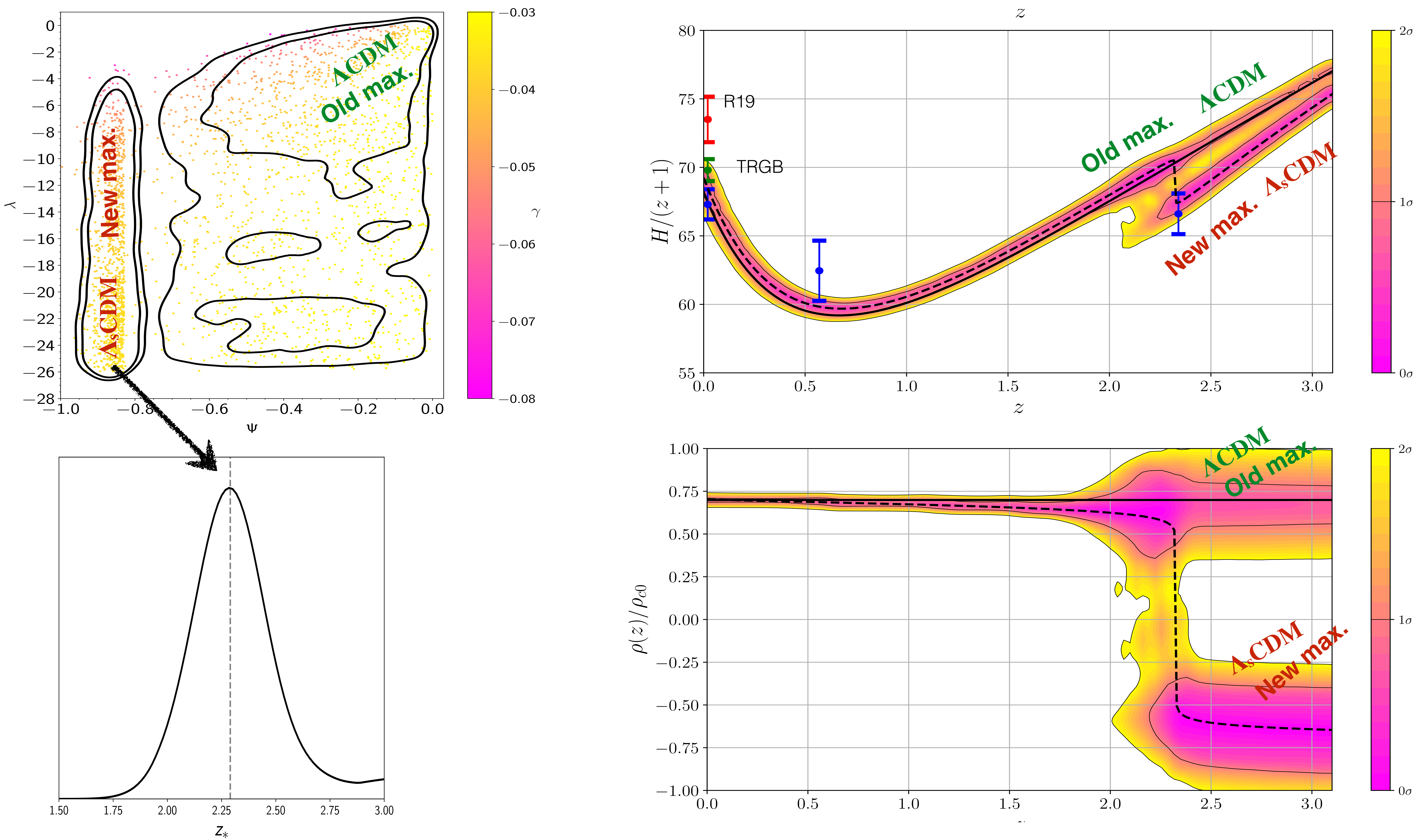

ΛCDM
Old max.
New max.
ΛsCDM
λ
Ψ
γ
z_*
z
$H/(z+1)$
R19
TRGB
$\rho(z)/\rho_{c0}$

Omnipotent dark energy: A phenomenological answer to the Hubble tension (Adil, Akarsu, Di Valentino, Nunes, Ozulker, Sen, Specogna, arXiv:2306.08046)

Density	EoS	Scaling in z	Scaling in a	Naming
$\rho > 0$	$w > -1$	$d\rho / dz > 0$	$d\rho / da < 0$	p-quintessence
	$w = -1$	$d\rho / dz = 0$	$d\rho / da = 0$	positive-CC
	$w < -1$	$d\rho / dz < 0$	$d\rho / da > 0$	p-phantom
$\rho < 0$	$w > -1$	$d\rho / dz < 0$	$d\rho / da > 0$	n-quintessence
	$w = -1$	$d\rho / dz = 0$	$d\rho / da = 0$	negative-CC
	$w < -1$	$d\rho / dz > 0$	$d\rho / da < 0$	n-phantom

An example: DMS20 parametrization, Di Valentino, Mukherjee & Sen, Entropy 2021, arXiv:2005.12587

$$\rho_{\rm DE}(a) = \rho_{\rm DE0}\frac{1+\alpha(a-a_m)^2+\beta(a-a_m)^3}{1+\alpha(1-a_m)^2+\beta(1-a_m)^3}$$

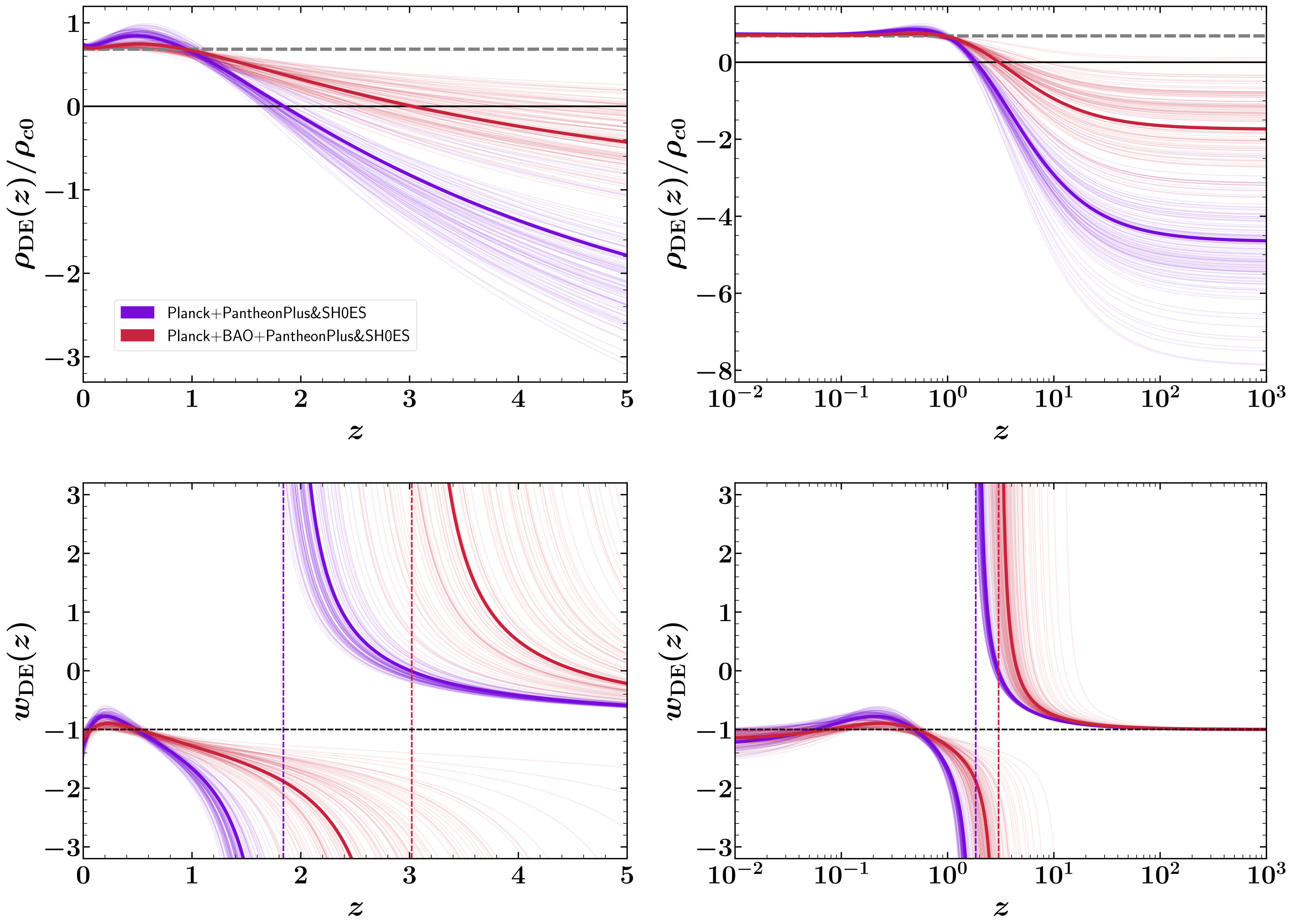

Model-independent reconstruction of the Interacting Dark Energy Kernel: Binned and Gaussian process (Escamilla, Akarsu, Di Valentino, Vazquez, arXiv:2305.16290)

See Luis' talk

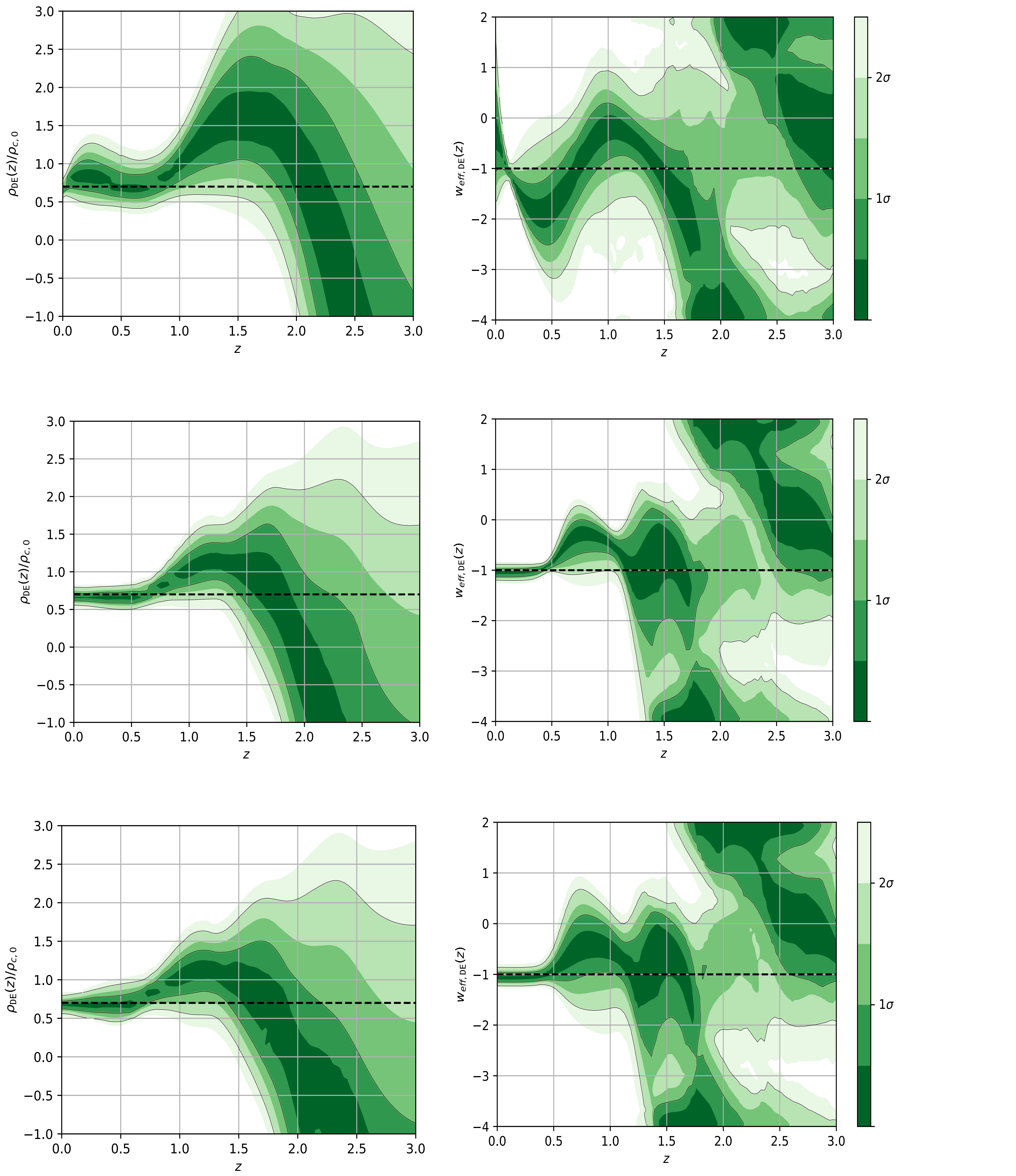

Some theoretical realizations…?

The meaning of imaginary space (Alexandre, Gielen & Magueijo arXiv:2306.11502)

They show that a classical metric signature change across boundaries with a degenerate metric in different formulations of general relativity allows for classical solutions where the open dS patch can arise from a portion of AdS space time.

$$\tilde{\Lambda} = \mathrm{sgn}(\tilde{a}^2)\Lambda$$

Constructing 4D Λ_sCDM models from the presence higher dimensions (Akarsu, Bulduk, Katırcı, Özülker, Perivolaropoulos, in progress)

$$ds^2 = -dt^2 + a^2(t)\,(dx_1^2 + dx_2^2 + dx_3^2) + s^2(t)\,\frac{dy_1^2 + \ldots + dy_n^2}{\left[1 + \frac{k_{\rm int}}{4}(y_1^2 + \ldots + y_n^2)\right]^2}$$

$$\tilde{T}_\mu^\nu = \mathrm{diag}[-\tilde{\rho}, \tilde{p}_{\rm ext}, \tilde{p}_{\rm ext}, \tilde{p}_{\rm ext}, \tilde{p}_{\rm int}, \ldots, \tilde{p}_{\rm int}]$$

$$\tilde{\chi} = \tilde{\Lambda} - \frac{n(n-1)}{2}\frac{k_{\rm int}}{s^2}$$

$$k_{\rm int} < 0$$

(Stability condition)

$$\tilde{w}_{\rm ext} = 0 \qquad \tilde{w}_{\rm int} = -\frac{1}{2} + \left(\frac{(n-1)(n+2)}{2\tilde{\kappa}}\frac{k_{\rm int}}{s_*^2} - \frac{\tilde{\Lambda}}{\tilde{\kappa}}\right)\frac{a^3}{\rho_{\rm m0}}.$$

$$a \to 0 \qquad \tilde{w}_{\rm ext} = 0 \qquad \tilde{w}_{\rm int} \to -\frac{1}{2}$$

$$G_{\rm 4D} \propto \frac{1}{V_{\rm int}} \propto \frac{\tilde{G}}{s^n} \longrightarrow \frac{G_{\rm 4D0}}{G_{\rm 4Dp}} = \left(\frac{s_{\rm p}}{s_0}\right)^n = \left(\frac{\tilde{\chi}_0 - \tilde{\Lambda}}{\tilde{\chi}_{\rm p} - \tilde{\Lambda}}\right)^{n/2}$$

(black strings/branes) Akarsu, Chopovsky, Zhuk, PLB 2018, arXiv:1711.08372: Satisfy the gravitational tests for the parameterized post-Newtonian parameter γ at the same level of accuracy as GR. Preferable from the thermodynamical point of view. Averaging over the Universe, they do not destroy the stabilization of the internal space.

?: Rapid transition of Geff at zt≃0.01 as a possible solution of the Hubble and growth tensions, Marra & Perivolaropoulos, PRD 2021, arXiv:2102.06012

Λ_sCDM MODEL: SIGN-SWITCHING Λ

$$\frac{\rho_{\rm DE}}{\rho_{\rm c,0}} \to \Omega_{\rm DE,0}\,{\rm sgn}[1-\Psi\ln a] \quad \text{as} \quad \lambda\to-\infty$$

$$\Lambda \quad \to \quad \Lambda_{\rm s}\equiv\Lambda_{\rm s0}\,{\rm sgn}[z_\dagger - z]$$

$$a(t)=\begin{cases} A^{\frac{1}{3}}\sin^{\frac{2}{3}}\left(\frac{3}{2}\sqrt{\frac{\Lambda_{\rm s0}}{3}}\,t\right) & \text{for} \quad t\le t_\dagger, \\ A^{\frac{1}{3}}\sinh^{\frac{2}{3}}\left[\frac{3}{2}\left(\sqrt{\frac{\Lambda_{\rm s0}}{3}}\,t+B\right)\right] & \text{for} \quad t\ge t_\dagger, \end{cases}$$

where

$$A=\sinh^{-2}\left[\frac{3}{2}\left(\sqrt{\frac{\Lambda_{\rm s0}}{3}}\,t_0+B\right)\right],$$

$$B={\rm arcsinh}\left[\sin\left(\frac{3}{2}\sqrt{\frac{\Lambda_{\rm s0}}{3}}\,t_\dagger\right)-\frac{3}{2}\sqrt{\frac{\Lambda_{\rm s0}}{3}}\,t_\dagger\right],$$

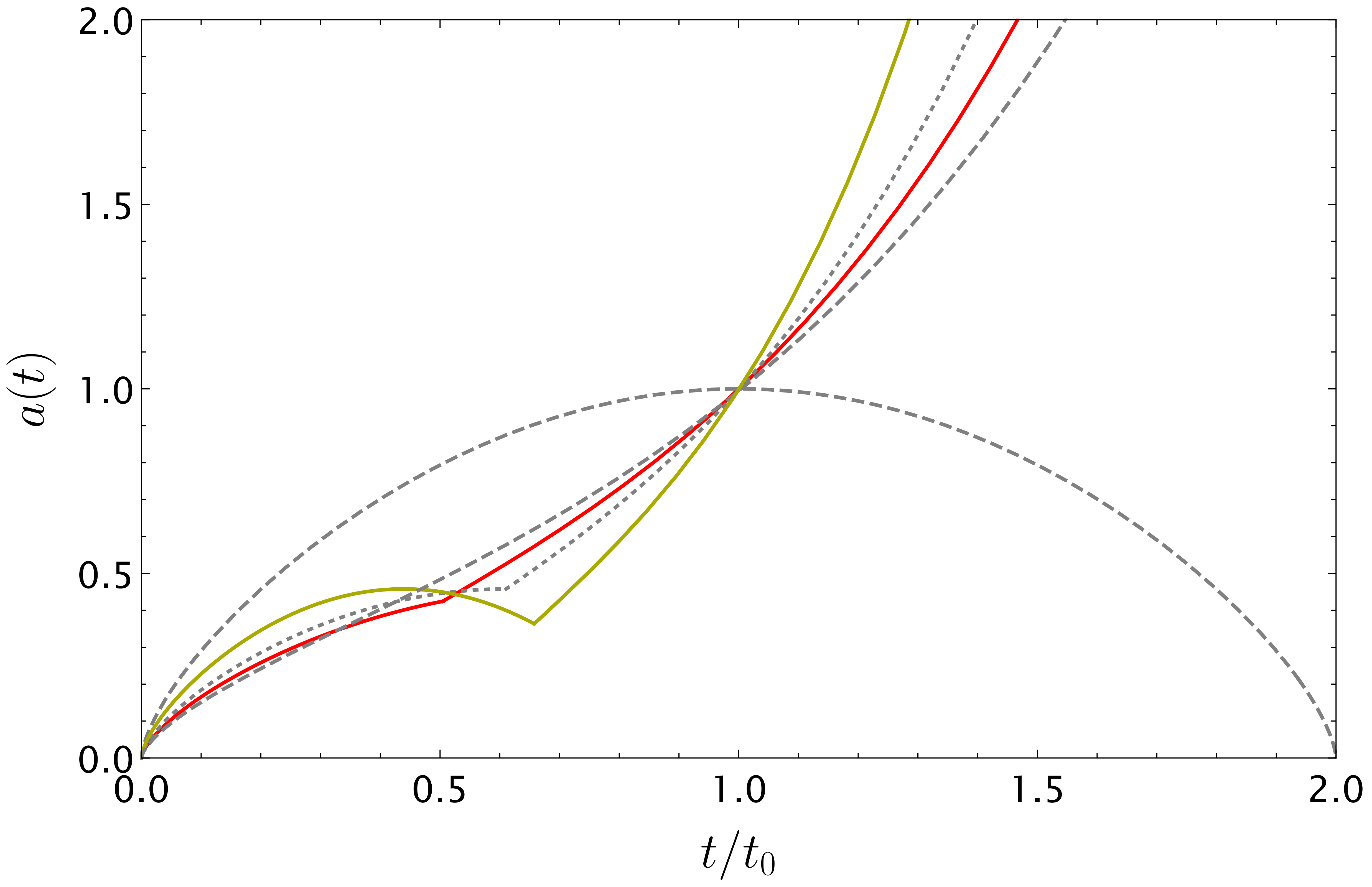

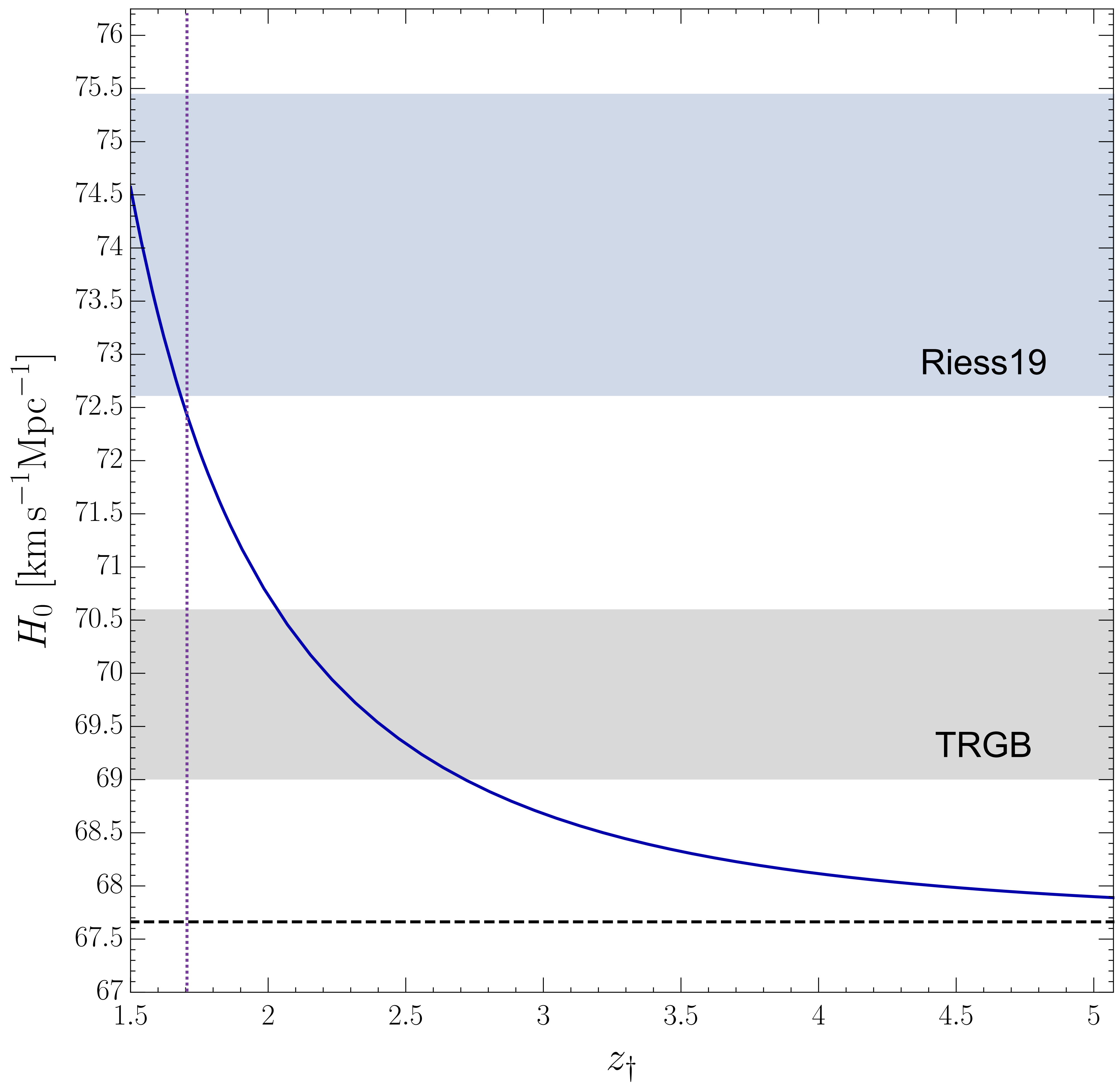

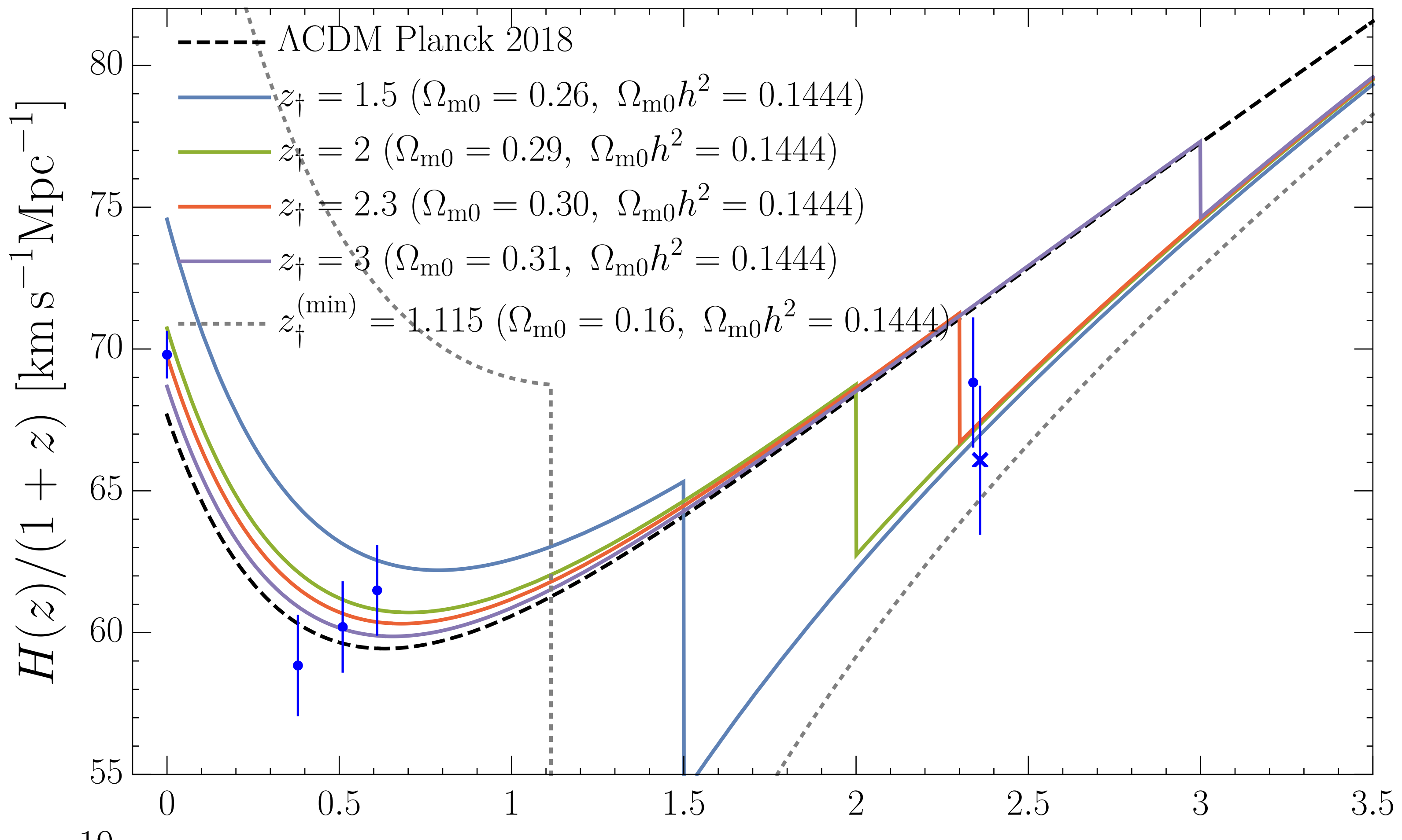

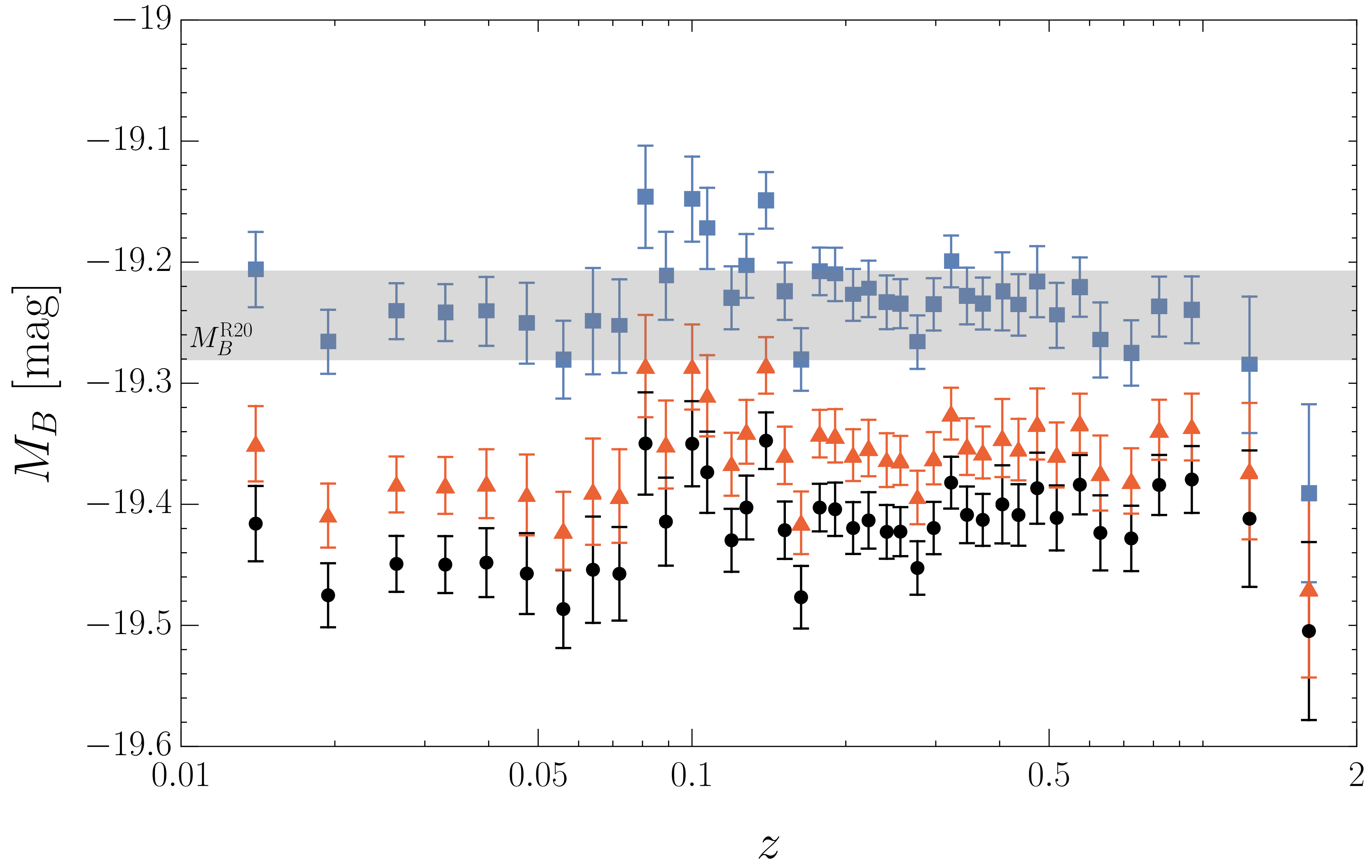

The figures are plotted by fixing $D_M(z_*)$ and $\rho_m(z_*)$ (and hence ρ_{m0}) to that of ΛCDM using the mean values of the *Planck* 2018 TT,TE,EE+lowE+lensing results.

Angular scale of the sound horizon at last scattering	Comoving sound horizon at last scattering	Comoving angular diameter distance out to last scattering
$$\theta_* = \frac{r_*}{D_M(z_*)}$$	$$r_* = \int_{z_*}^{\infty} \frac{c_s(z)}{H_{\Lambda CDM}(z)}\,dz$$	$$D_M(z_*) = c\int_0^{z_*} \frac{dz}{H(z)}$$
$100\theta_* = 1.04110 \pm 0.00031$ (ΛCDM PL18)	$r_* = 144.43 \pm 0.26$ Mpc (ΛCDM PL18)	$D_{M(z*)} = 13872.83 \pm 25.31$ Mpc (ΛCDM PL18)

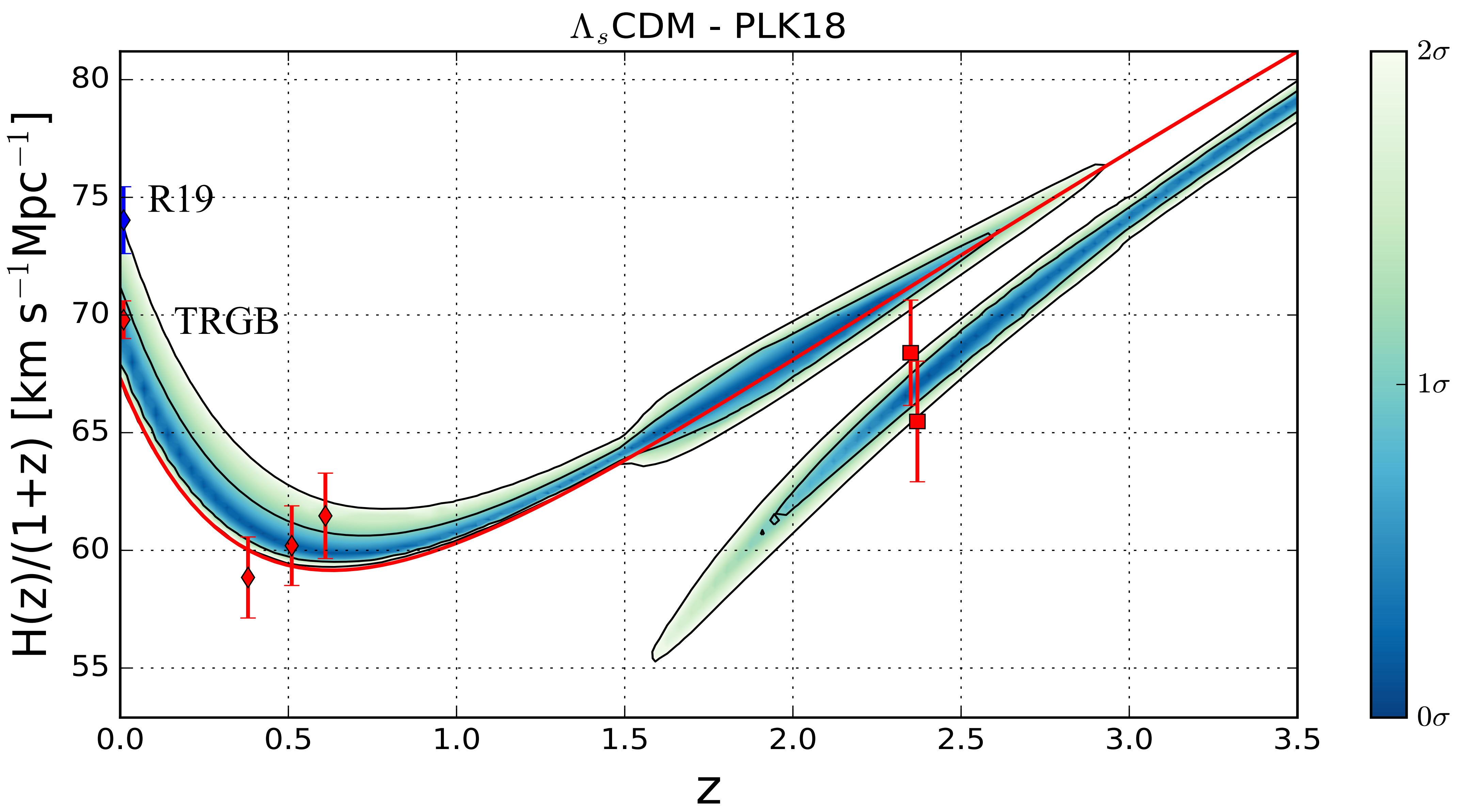

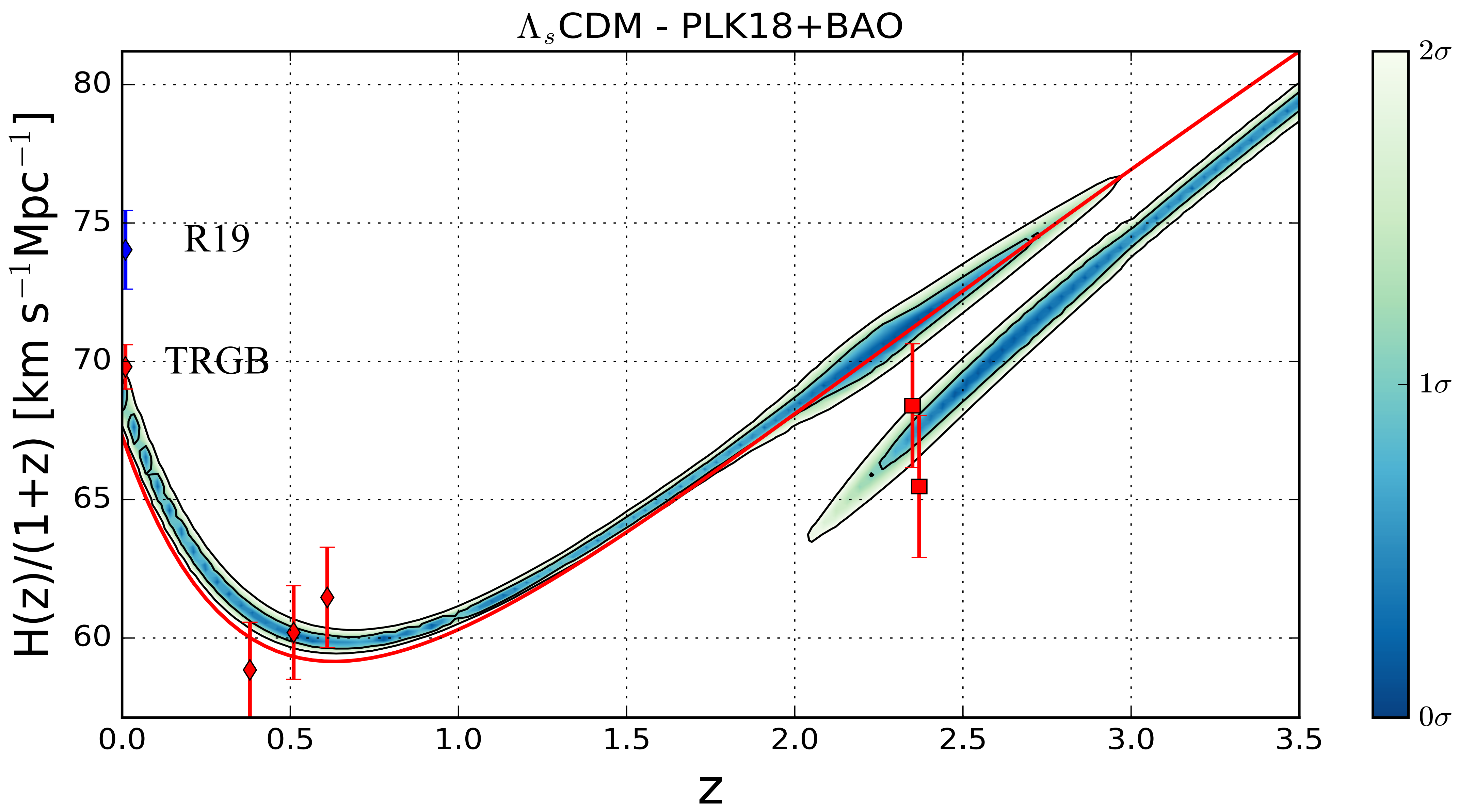

Data set	**CMB**			**CMB+BAO**		
	ΛCDM	**Λ_sCDM**	**Λ_sCDM+$z_\dagger = 2.32$**	**ΛCDM**	**Λ_sCDM**	**Λ_sCDM+$z_\dagger = 2.32$**
$10^2\omega_b$	2.235 ± 0.015	2.238 ± 0.015	2.238 ± 0.015	2.244 ± 0.013	2.231 ± 0.014	2.230 ± 0.013
ω_c	0.1201 ± 0.0014	0.1197 ± 0.0013	0.1199 ± 0.0013	0.1189 ± 0.0009	0.1208 ± 0.0011	0.1209 ± 0.0009
$100\theta_s$	1.04090 ± 0.00031	1.04093 ± 0.00030	1.04091 ± 0.00031	1.04102 ± 0.00029	1.04081 ± 0.00029	1.04080 ± 0.00029
$\ln(10^{10}A_s)$	3.044 ± 0.016	3.043 ± 0.016	3.043 ± 0.016	3.045 ± 0.016	3.043 ± 0.016	3.043 ± 0.016
n_s	0.9646 ± 0.0043	0.9657 ± 0.0044	0.9655 ± 0.0044	0.9673 ± 0.0037	0.9633 ± 0.0039	0.9632 ± 0.0036
τ_{reio}	0.0543 ± 0.0078	0.0542 ± 0.0078	0.0541 ± 0.0078	0.0559 ± 0.0078	0.0530 ± 0.0077	0.0526 ± 0.0075
$z_\dagger$	—	unconstrained	[2.32]	—	2.44 ± 0.29	[2.32]
Ω_m	0.3162 ± 0.0084	0.2900 ± 0.0160	0.2967 ± 0.0086	0.3090 ± 0.0059	0.3035 ± 0.0062	0.3029 ± 0.0060
H_0	67.29 ± 0.60	70.22 ± 1.78	69.42 ± 0.71	67.81 ± 0.44	68.82 ± 0.55	68.91 ± 0.48
σ_8	0.8117 ± 0.0076	0.8223 ± 0.0098	0.8186 ± 0.0074	0.8090 ± 0.0073	0.8207 ± 0.0080	0.8215 ± 0.0071
S_8	0.8332 ± 0.0163	0.8071 ± 0.0210	0.8138 ± 0.0166	0.8219 ± 0.0127	0.8255 ± 0.0128	0.8264 ± 0.0126
$-2\ln\mathcal{L}_{max}$	1386.52	1385.73	1386.56	1394.32	1393.77	1393.54
$\ln\mathcal{Z}$	−1424.19	−1424.22	−1423.50	−1431.46	−1432.77	−1431.89
$\Delta\ln\mathcal{Z}$	0.69	0.72	0	0	1.31	0.43

ΛsCDM - PLK18
ΛsCDM - PLK18+BAO
R19
TRGB
H(z)/(1+z) [km s^-1 Mpc^-1]
z
0σ
1σ
2σ
PLK18
PLK18+BAO
Riess19
TRGB
ΛCDM (PLK18+BAO)
H0[kms^-1Mpc^-1]
z†
ΛsCDM
ΛsCDM + z†
ΛCDM
S8
Ωm
ΛCDM
ΛsCDM
ΛsCDM + z† = 2.32
M_B^R20
M_B = −19.244±0.037 mag
M_B [mag]
CMB

Relaxing cosmological tensions with a sign switching cosmological constant: Improved results with Planck, BAO and Pantheon data

Akarsu, Kumar, Özülker, Vazquez & Yadav, PRD (2023), arXiv:2108.09239

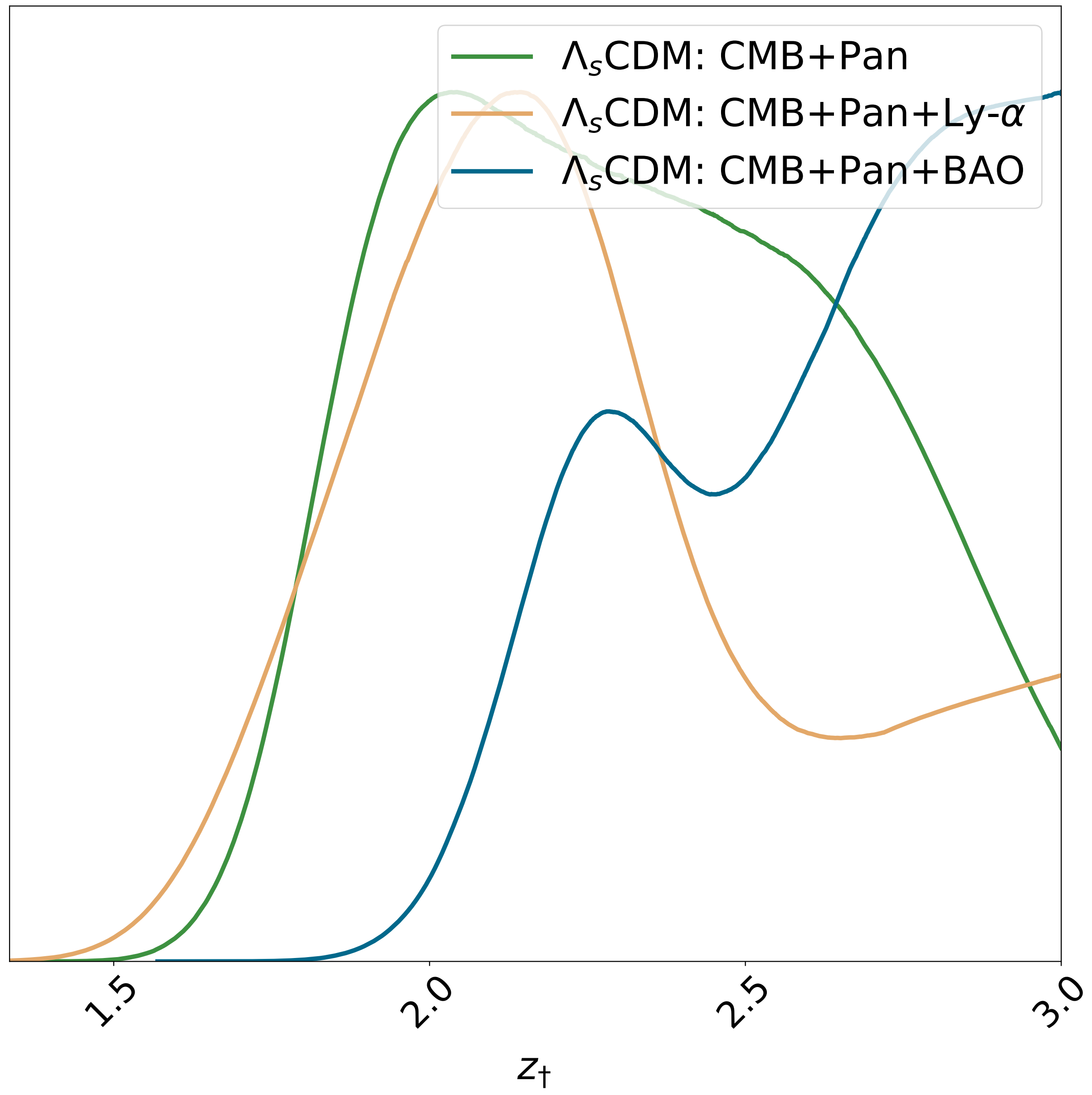

Data set	CMB+Pan		CMB+Pan+Ly-α		CMB+Pan+BAO	
	ΛCDM	Λ_sCDM	ΛCDM	Λ_sCDM	ΛCDM	Λ_sCDM
$10^2\omega_b$	2.240 ± 0.015	2.241 ± 0.014	2.242 ± 0.013	2.241 ± 0.015	2.242 ± 0.013	2.235 ± 0.014
ω_c	0.1197 ± 0.0012	0.1196 ± 0.0011	0.1193 ± 0.0009	0.1196 ± 0.0011	0.1193 ± 0.0009	0.1206 ± 0.0010
$100\theta_s$	1.04191 ± 0.00029	1.04190 ± 0.00028	1.04191 ± 0.00029	1.04190 ± 0.00029	1.04194 ± 0.00028	1.04180 ± 0.00030
$\ln(10^{10}A_s)$	3.047 ± 0.015	3.041 ± 0.014	3.047 ± 0.014	3.040 ± 0.015	3.047 ± 0.015	3.040 ± 0.014
n_s	0.9662 ± 0.0042	0.9668 ± 0.0040	$0.9669^{+0.0039}_{-0.0036}$	0.9668 ± 0.0041	0.9665 ± 0.0037	0.9644 ± 0.0037
τ_{reio}	0.0556 ± 0.0075	0.0533 ± 0.0075	0.0560 ± 0.0069	0.0528 ± 0.0077	0.0561 ± 0.0076	0.0515 ± 0.0073
$z_\dagger$	—	> 1.80 (95% CL)	—	$2.21^{+0.16}_{-0.38}$	—	> 2.13 (95% CL)
M_B [mag]	-19.421 ± 0.014	$-19.363^{+0.021}_{-0.037}$	-19.418 ± 0.011	-19.349 ± 0.028	-19.418 ± 0.012	-19.387 ± 0.015
Ω_m	0.3129 ± 0.0071	$0.2940^{+0.0120}_{-0.0093}$	0.3110 ± 0.0053	0.2899 ± 0.0097	0.3109 ± 0.0056	0.3039 ± 0.0058
ω_m	0.1427 ± 0.0011	0.1427 ± 0.0010	0.1424 ± 0.0008	0.1426 ± 0.0010	0.1424 ± 0.0009	0.1436 ± 0.0010
H_0 [km/s/Mpc]	67.55 ± 0.53	$69.68^{+0.77}_{-1.40}$	67.68 ± 0.40	$70.17^{+0.96}_{-1.10}$	$67.69^{+0.38}_{-0.43}$	$68.74^{+0.49}_{-0.55}$
t_0 [Gyr]	13.79 ± 0.02	$13.65^{+0.06}_{-0.04}$	13.79 ± 0.02	$13.62^{+0.09}_{-0.03}$	13.79 ± 0.02	$13.71^{+0.03}_{-0.02}$
σ_8	$0.8111^{+0.0056}_{-0.0063}$	$0.8167^{+0.0059}_{-0.0067}$	0.8104 ± 0.0060	0.8182 ± 0.0066	0.8101 ± 0.0063	0.8167 ± 0.0062
S_8	0.828 ± 0.013	0.809 ± 0.015	0.825 ± 0.010	0.804 ± 0.014	0.825 ± 0.011	0.822 ± 0.010
$-2\ln\mathcal{L}_{max}$	1903.62	1902.50	1909.68	1903.44	1909.63	1909.53
$\ln\mathcal{Z}$	-1937.82	-1938.02	-1944.53	-1939.75	-1944.51	-1944.76
$\Delta\ln\mathcal{Z}$	0	0.20	4.78	0	0	0.25

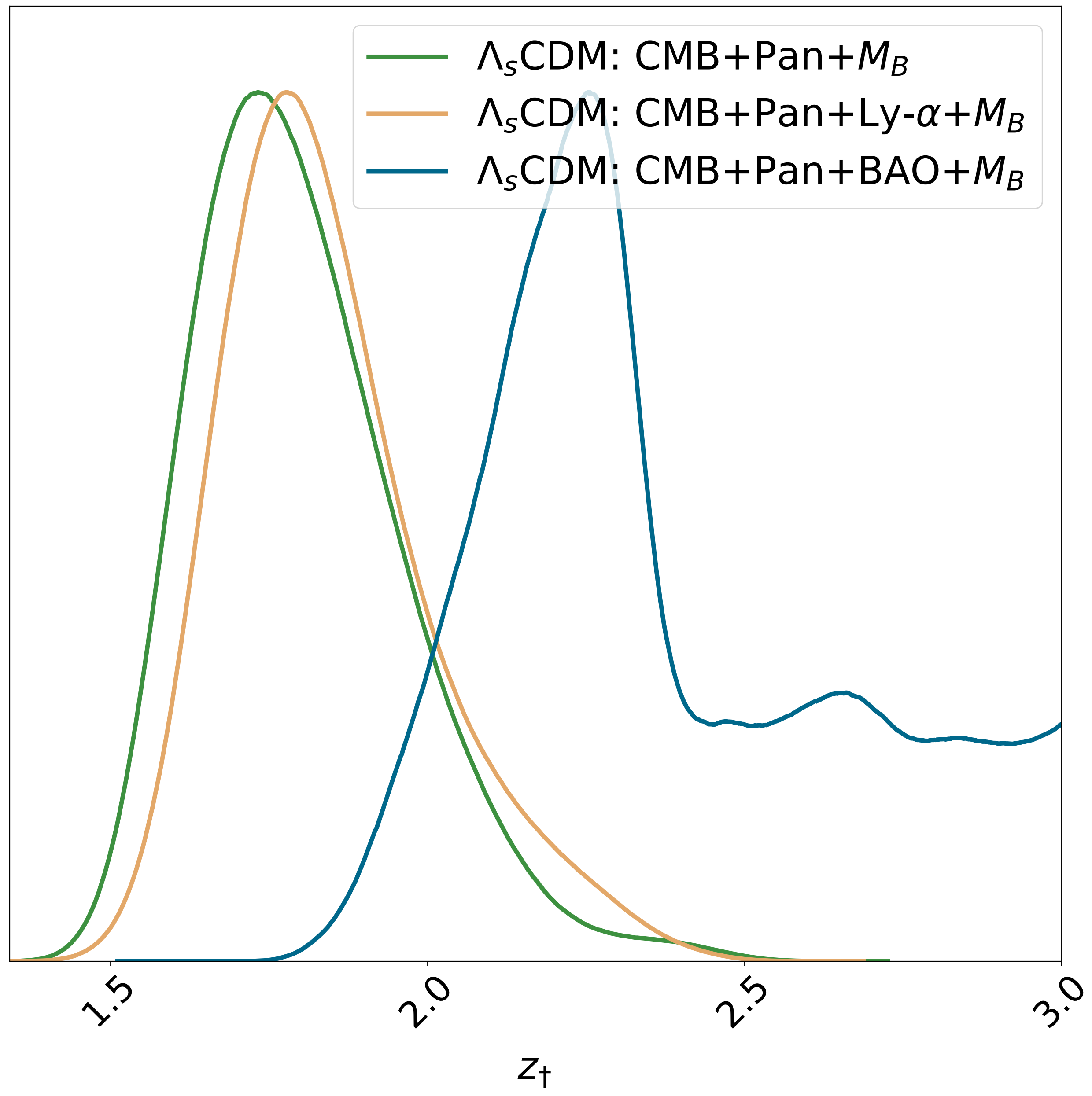

Data set	CMB+Pan+M_B		CMB+Pan+Ly-α+M_B		CMB+Pan+BAO+M_B	
	ΛCDM	Λ_sCDM	ΛCDM	Λ_sCDM	ΛCDM	Λ_sCDM
$10^2\omega_b$	2.256 ± 0.015	2.248 ± 0.014	2.253 ± 0.013	$2.247^{+0.014}_{-0.013}$	2.255 ± 0.013	2.242 ± 0.014
ω_c	0.1181 ± 0.0011	0.1191 ± 0.0011	0.1183 ± 0.0008	0.1191 ± 0.0011	0.1181 ± 0.0009	$0.1200^{+0.0010}_{-0.0011}$
$100\theta_s$	1.04208 ± 0.00029	1.04197 ± 0.00031	1.04204 ± 0.00028	1.04196 ± 0.00028	$1.04207^{+0.00029}_{-0.00026}$	1.04186 ± 0.00028
$\ln(10^{10}A_s)$	$3.053^{+0.014}_{-0.017}$	3.039 ± 0.014	$3.052^{+0.013}_{-0.016}$	3.041 ± 0.015	$3.053^{+0.014}_{-0.016}$	3.041 ± 0.015
n_s	0.9701 ± 0.0040	$0.9687^{+0.0043}_{-0.0038}$	0.9697 ± 0.0035	0.9684 ± 0.0041	0.9702 ± 0.0035	0.9661 ± 0.0037
τ_{reio}	$0.0601^{+0.0072}_{-0.0085}$	0.0526 ± 0.0074	$0.0593^{+0.0064}_{-0.0079}$	0.0535 ± 0.0077	$0.0603^{+0.0070}_{-0.0078}$	0.0524 ± 0.0076
$z_\dagger$	—	$1.78^{+0.14}_{-0.18}$	—	$1.84^{+0.13}_{-0.21}$	—	2.36 ± 0.28
M_B [mag]	-19.399 ± 0.014	$-19.290^{+0.026}_{-0.029}$	-19.402 ± 0.011	-19.299 ± 0.028	-19.399 ± 0.011	$-19.366^{+0.013}_{-0.015}$
Ω_m	0.3028 ± 0.0068	0.2716 ± 0.0084	0.3043 ± 0.0050	$0.2743^{+0.0086}_{-0.0097}$	0.3030 ± 0.0051	0.2965 ± 0.0055
ω_m	0.1413 ± 0.0011	0.1422 ± 0.0010	0.1415 ± 0.0008	0.1422 ± 0.0011	0.1413 ± 0.0008	0.1431 ± 0.0010
H_0 [km/s/Mpc]	68.31 ± 0.52	$72.38^{+0.98}_{-1.10}$	68.19 ± 0.38	72.0 ± 1.1	68.29 ± 0.39	$69.48^{+0.48}_{-0.55}$
t_0 [Gyr]	13.76 ± 0.02	13.55 ± 0.05	13.76 ± 0.02	$13.56^{+0.04}_{-0.04}$	13.76 ± 0.02	13.67 ± 0.03
σ_8	0.8090 ± 0.0064	$0.8255^{+0.0072}_{-0.0081}$	$0.8091^{+0.0054}_{-0.0063}$	0.8243 ± 0.0076	$0.8092^{+0.0057}_{-0.0061}$	0.8176 ± 0.0063
S_8	0.813 ± 0.012	0.785 ± 0.012	0.815 ± 0.010	$0.788^{+0.012}_{-0.014}$	0.813 ± 0.010	0.813 ± 0.010
$-2\ln\mathcal{L}_{max}$	1913.28	1904.29	1918.68	1905.88	1919.85	1915.57
$\ln\mathcal{Z}$	-1947.83	-1940.06	-1954.17	-1941.85	-1955.02	-1951.79
$\Delta\ln\mathcal{Z}$	7.77	0	12.32	0	3.23	0

Data set	CMB+Pan		CMB+Pan+Ly-α		CMB+Pan+BAO		CMB+Pan+M_B		CMB+Pan+Ly-α+M_B		CMB+Pan+BAO+M_B	
	ΛCDM	Λ_sCDM	ΛCDM	Λ_sCDM	ΛCDM	Λ_sCDM	ΛCDM	Λ_sCDM	ΛCDM	Λ_sCDM	ΛCDM	Λ_sCDM
$H_0^{\rm R21}$	4.7σ	2.2σ	4.8σ	2.0σ	4.8σ	3.7σ	4.1σ	0.4σ	4.4σ	0.7σ	4.3σ	3.1σ
$H_0^{\rm TRGB}$	2.3σ	0.1σ	2.8σ	0.3σ	2.4σ	1.1σ	1.6σ*	2.0σ*	1.8σ*	1.6σ*	1.7σ*	0.3σ*
M_B (SH0ES)	4.5σ	2.5σ	4.5σ	2.3σ	4.5σ	3.6σ	3.9σ	1.0σ	4.1σ	1.2σ	4.0σ	3.1σ
S_8 (KiDS)	2.9σ	1.9σ	3.0σ	1.7σ	2.9σ	2.8σ	2.3σ	0.9σ	2.5σ	1.0σ	2.4σ	2.4σ
$D_H(2.33)/r_{\rm d}$	2.0σ	0.2σ	1.9σ	0.1σ	1.9σ	1.1σ	1.9σ	1.2σ	1.8σ	1.2σ	1.9σ	0.1σ
$t_{\rm u}$	1.9σ	1.0σ	1.9σ	0.8σ	1.9σ	1.4σ	1.7σ	0.3σ	1.7σ	0.4σ	1.7σ	1.1σ
$\omega_{\rm b}^{\rm PCUV21}$	1.7σ	1.8σ	1.8σ	1.7σ	1.8σ	1.5σ	2.3σ	2.0σ	2.3σ	2.0σ	2.3σ	1.8σ
$\omega_{\rm b}^{\rm LUNA}$	0.2σ	0.2σ	0.2σ	0.2σ	0.2σ	0.1σ	0.6σ	0.4σ	0.5σ	0.4σ	0.6σ	0.2σ

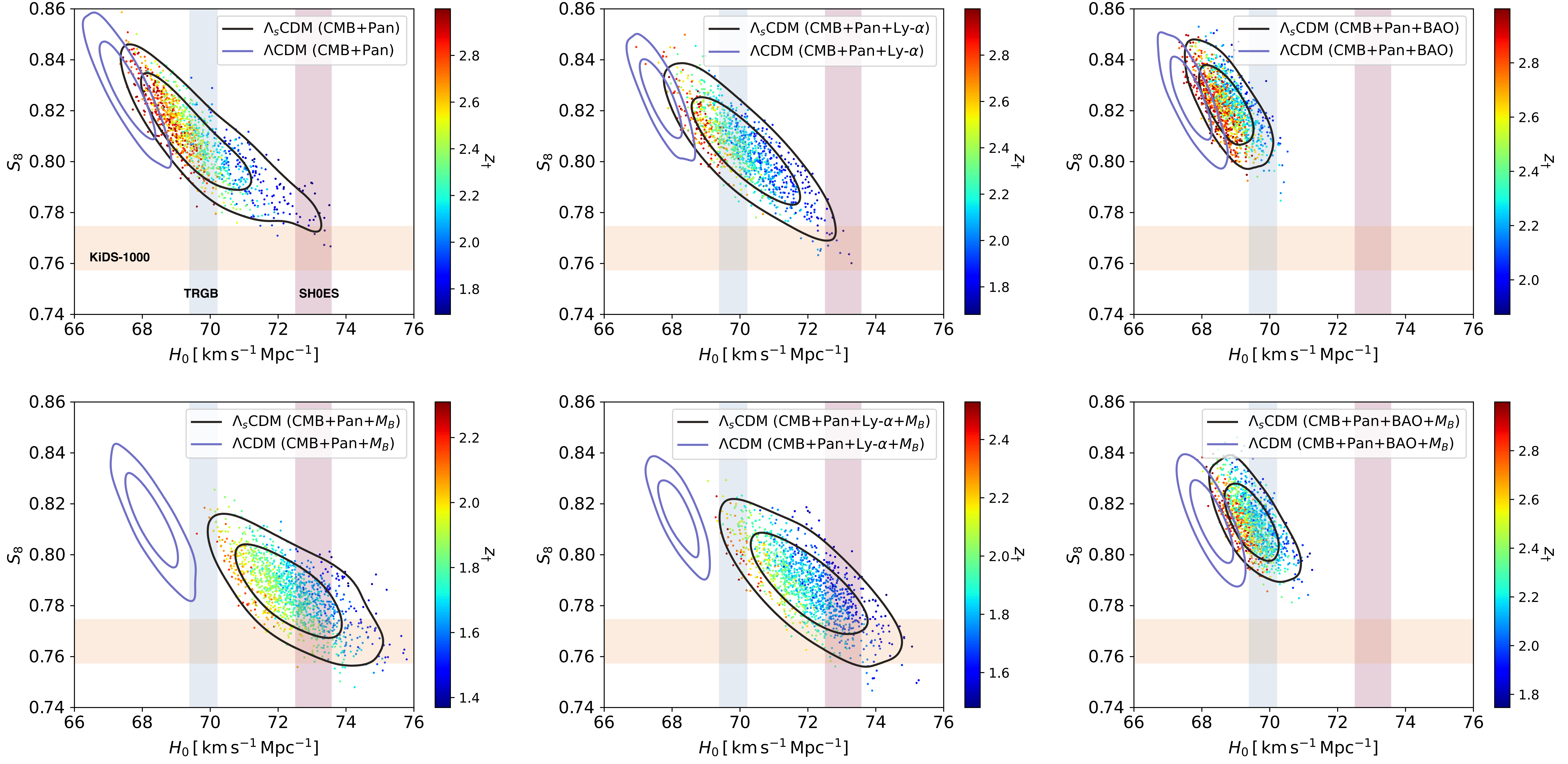

Λ_sCDM (CMB+Pan)
ΛCDM (CMB+Pan)
KiDS-1000
TRGB
SH0ES
Λ_sCDM (CMB+Pan+Ly-α)
ΛCDM (CMB+Pan+Ly-α)
Λ_sCDM (CMB+Pan+BAO)
ΛCDM (CMB+Pan+BAO)
Λ_sCDM (CMB+Pan+M_B)
ΛCDM (CMB+Pan+M_B)
Λ_sCDM (CMB+Pan+Ly-α+M_B)
ΛCDM (CMB+Pan+Ly-α+M_B)
Λ_sCDM (CMB+Pan+BAO+M_B)
ΛCDM (CMB+Pan+BAO+M_B)
S_8
$H_0\,[\mathrm{km\,s^{-1}\,Mpc^{-1}}]$
$z_\dagger$

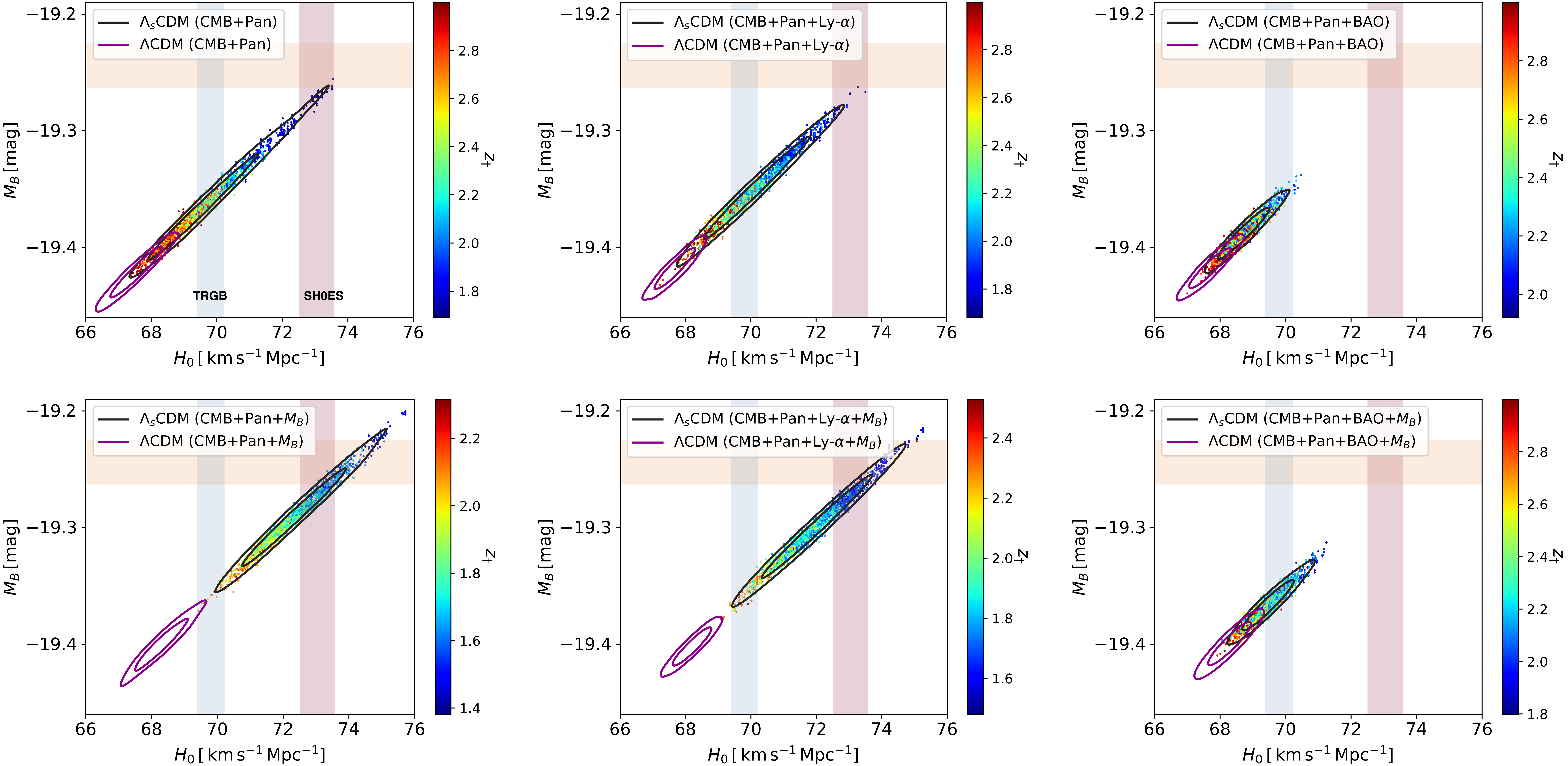

ΛsCDM (CMB+Pan)
ΛCDM (CMB+Pan)
TRGB
SH0ES
ΛsCDM (CMB+Pan+Ly-α)
ΛCDM (CMB+Pan+Ly-α)
ΛsCDM (CMB+Pan+BAO)
ΛCDM (CMB+Pan+BAO)
ΛsCDM (CMB+Pan+M_B)
ΛCDM (CMB+Pan+M_B)
ΛsCDM (CMB+Pan+Ly-α+M_B)
ΛCDM (CMB+Pan+Ly-α+M_B)
ΛsCDM (CMB+Pan+BAO+M_B)
ΛCDM (CMB+Pan+BAO+M_B)
M_B [mag]
H_0 [km s^-1 Mpc^-1]
z†

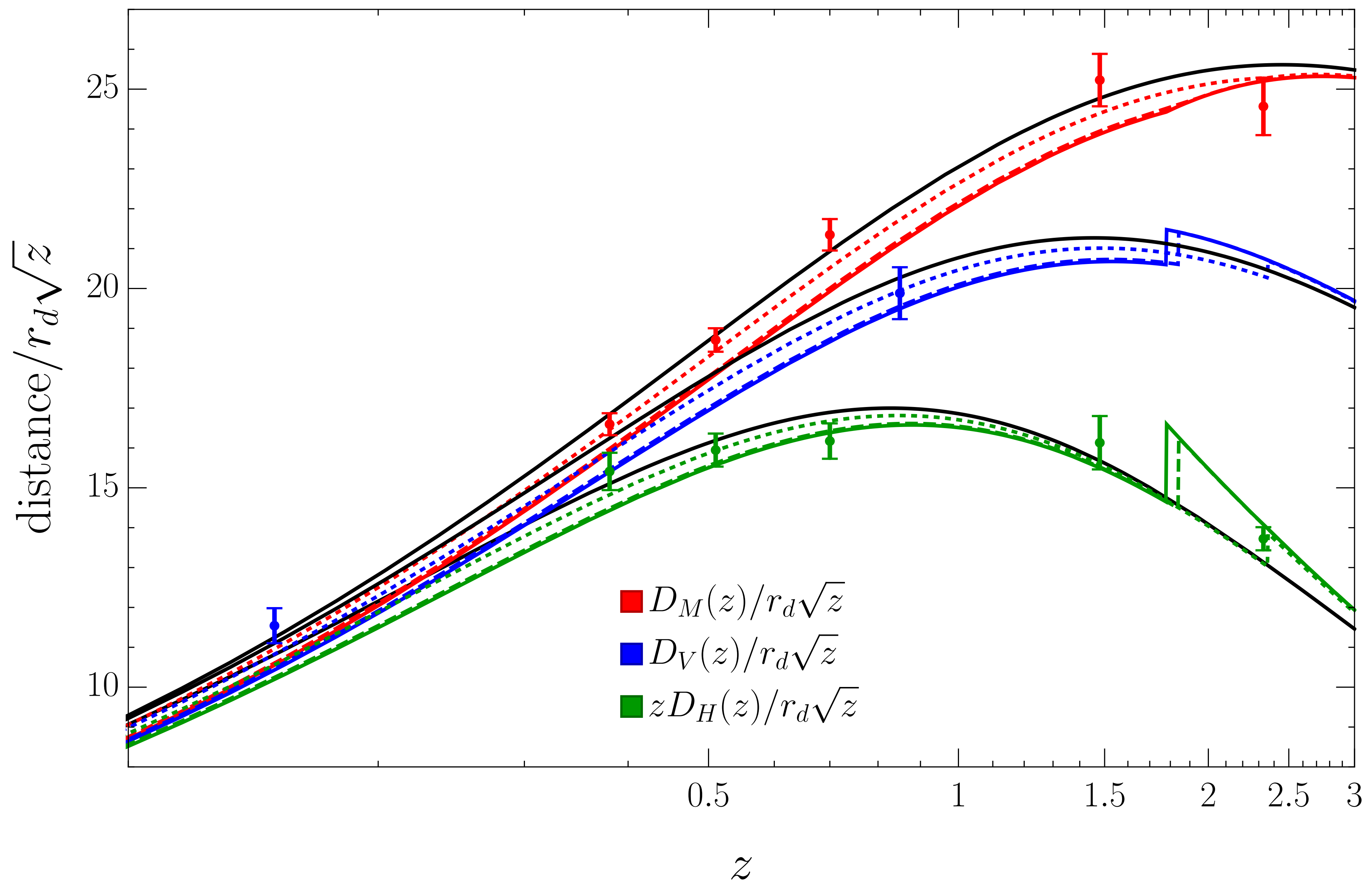

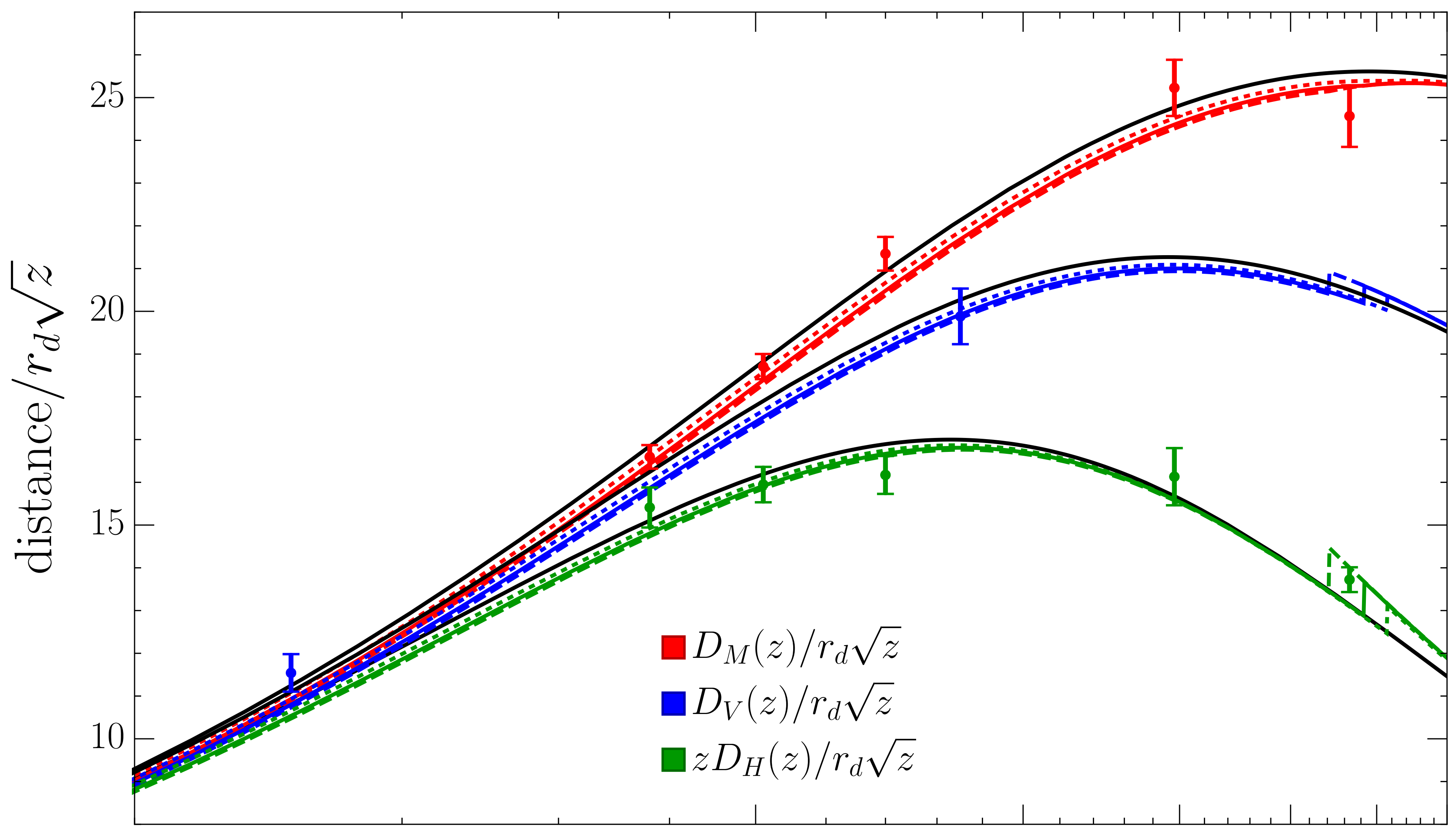

Data set	**CMB+Pan**		**CMB+Pan+Ly-α**		**CMB+Pan+BAO**		**CMB+Pan+M_B**		**CMB+Pan+Ly-α+M_B**		**CMB+Pan+BAO+M_B**	
	ΛCDM	**Λ_sCDM**	**ΛCDM**	**Λ_sCDM**	**ΛCDM**	**Λ_sCDM**	**ΛCDM**	**Λ_sCDM**	**ΛCDM**	**Λ_sCDM**	**ΛCDM**	**Λ_sCDM**
$D_V(0.15)/r_d$	0.9σ	1.7σ	1.0σ	1.8σ	1.0σ	0.7σ	1.2σ	2.4σ	1.3σ	2.3σ	1.2σ	1.6σ
$D_V(0.85)/r_d$	0.7σ	0.0σ	0.6σ	0.1σ	0.6σ	0.3σ	0.5σ	0.6σ	0.4σ	0.5σ	0.5σ	0.2σ
$D_M(0.38)/r_d$	0.9σ	0.6σ	0.9σ	0.9σ	0.8σ	0.2σ	0.3σ	2.0σ	0.3σ	1.8σ	0.4σ	0.3σ
$D_M(0.51)/r_d$	0.5σ	0.9σ	0.4σ	1.2σ	0.4σ	0.3σ	0.1σ	2.3σ	0.1σ	2.2σ	0.0σ	0.8σ
$D_M(0.70)/r_d$	0.9σ	1.9σ	0.9σ	2.1σ	1.0σ	1.5σ	1.3σ	3.1σ	1.4σ	3.0σ	1.3σ	2.0σ
$D_M(1.48)/r_d$	0.6σ	1.3σ	0.6σ	1.5σ	0.7σ	1.0σ	0.8σ	1.9σ	0.9σ	1.9σ	0.8σ	1.2σ
$D_M(2.33)/r_d$	1.5σ	1.0σ	1.5σ	1.0σ	1.5σ	1.2σ	1.3σ	0.9σ	1.3σ	0.9σ	1.4σ	1.1σ
$D_H(0.38)/r_d$	0.6σ	1.3σ	0.6σ	1.4σ	0.6σ	0.9σ	0.8σ	2.0σ	0.9σ	1.9σ	0.8σ	1.2σ
$D_H(0.51)/r_d$	0.7σ	0.1σ	0.6σ	0.3σ	0.6σ	0.3σ	0.4σ	0.8σ	0.4σ	0.8σ	0.4σ	0.0σ
$D_H(0.70)/r_d$	1.7σ	1.0σ	1.7σ	0.9σ	1.7σ	1.4σ	1.5σ	0.5σ	1.5σ	0.5σ	1.5σ	1.2σ
$D_H(1.48)/r_d$	0.6σ	0.8σ	0.6σ	0.8σ	0.6σ	0.7σ	0.6σ	0.9σ	0.6σ	0.9σ	0.6σ	0.8σ
$D_H(2.33)/r_d$	2.0σ	0.2σ	1.9σ	0.1σ	1.9σ	1.1σ	1.9σ	1.2σ	1.8σ	1.2σ	1.9σ	0.1σ

Λ_sCDM model: A promising scenario for alleviation of cosmological tensions

Akarsu, Di Valentino, Kumar, Nunes, Vazquez & Yadav, arXiv:2307.10899

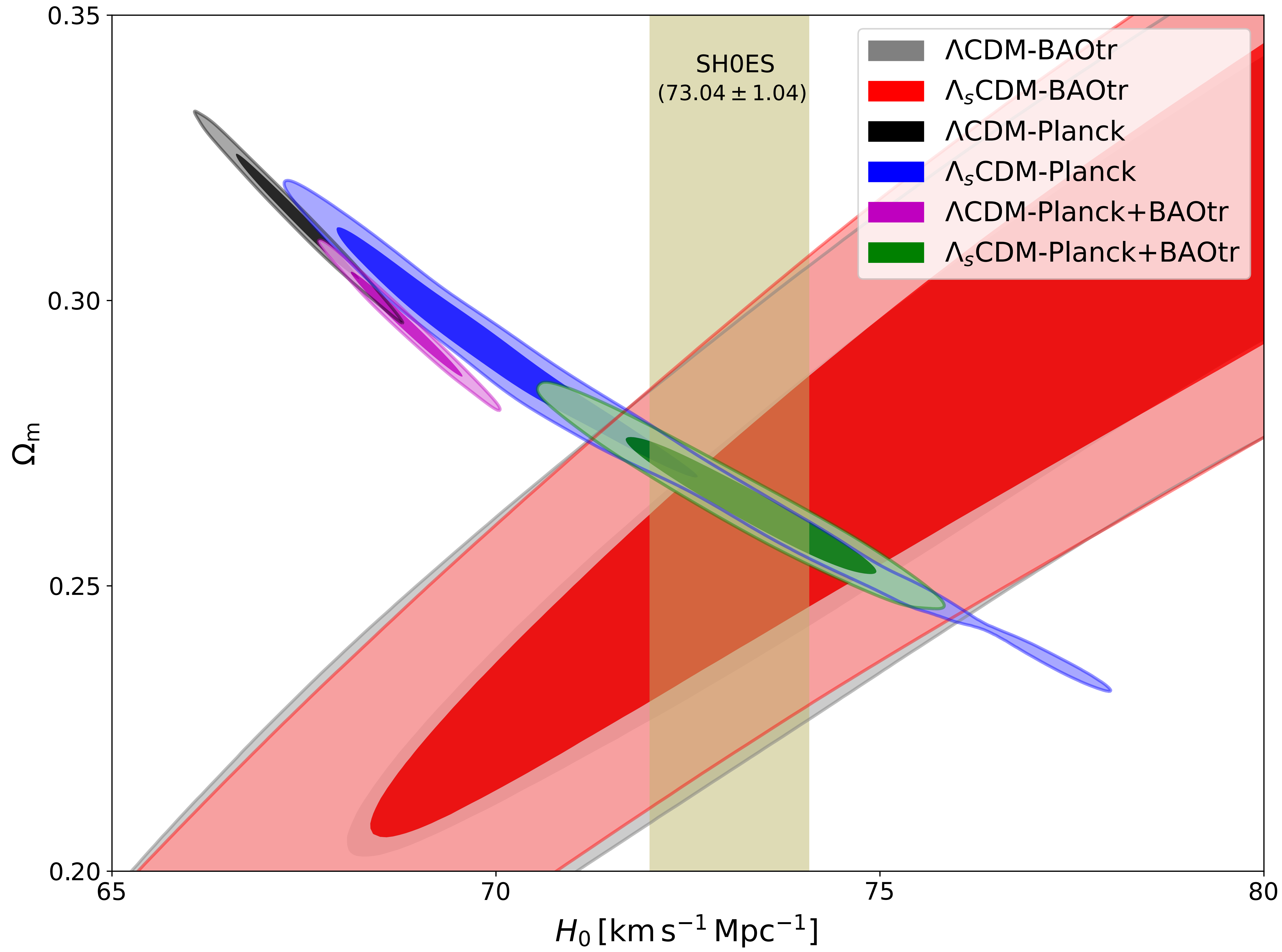

Here **BAOtr** dataset is the **2D BAO** dataset (less model independent) compiled in arXiv:2002.09293 (Nunes, Yadav, Jesus, Bernui, MNRAS 2020) and arXiv:2103.14121 (Carvalho, Bernui, Avila, Novaes, Nogueira-Cavalcante, A&A 2021)

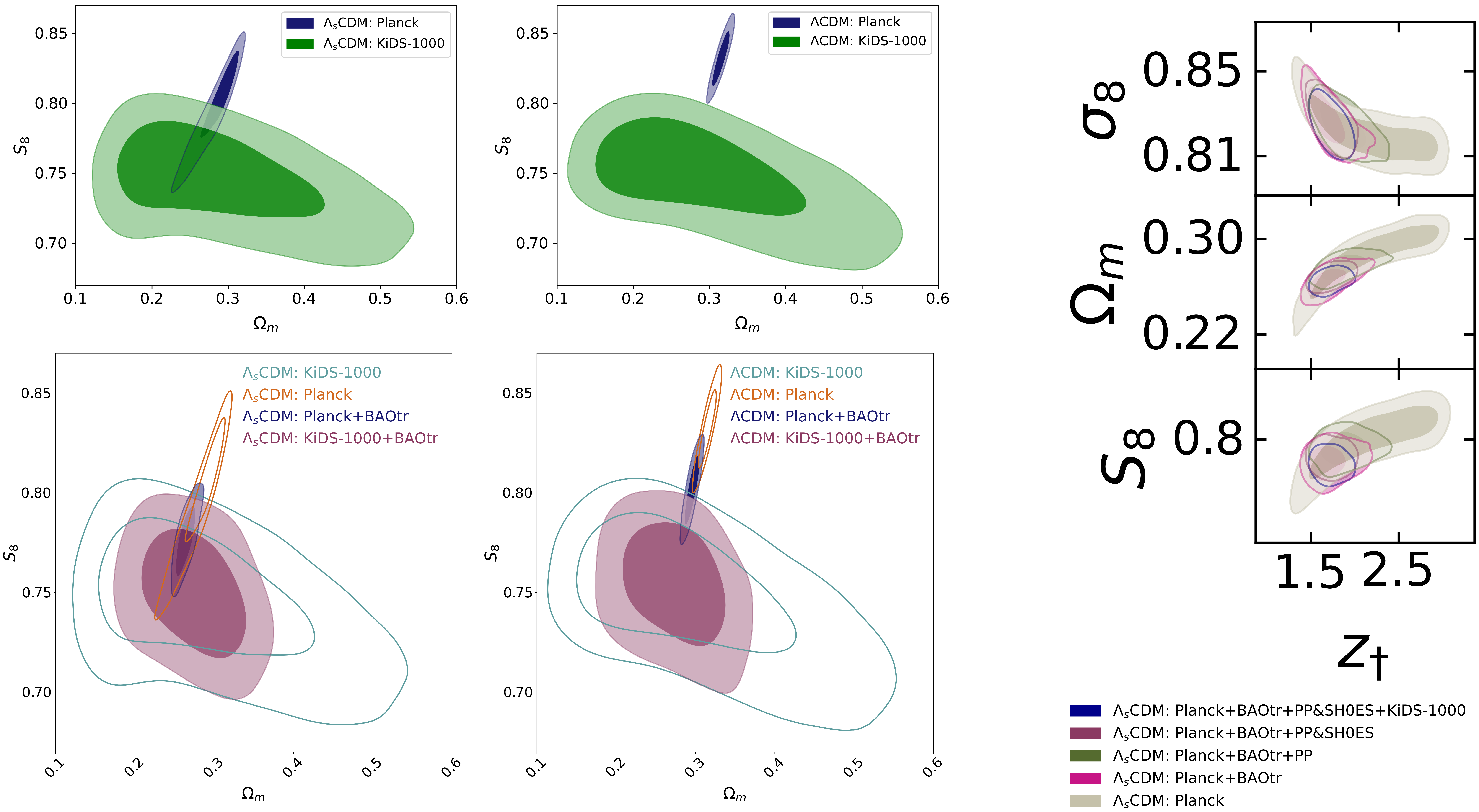

FIG. 1. 2D contours at 68%, and 95% CLs in the $\Omega_{\rm m}$-S_8 plane for the Λ_sCDM and ΛCDM models. $S_8 = 0.801^{+0.026}_{-0.016}$ (Λ_sCDM: Planck), $S_8 = 0.746^{+0.026}_{-0.021}$ (Λ_sCDM: KiDS), $S_8 = 0.832 \pm 0.012$ (ΛCDM: Planck), $S_8 = 0.749^{+0.027}_{-0.020}$ (ΛCDM: KiDS) at 68% CL.

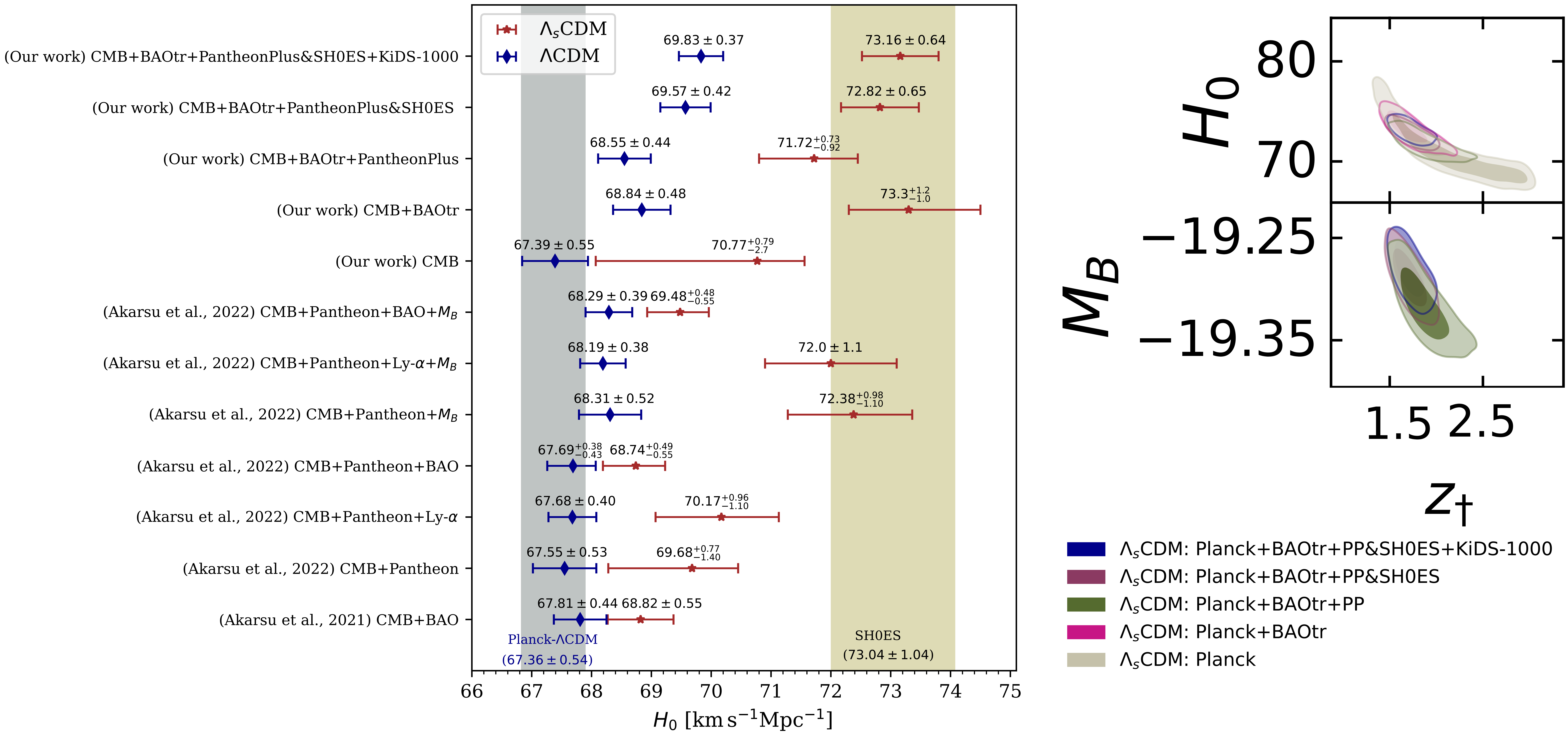

(Our work) CMB+BAOtr+PantheonPlus&SH0ES+KiDS-1000
(Our work) CMB+BAOtr+PantheonPlus&SH0ES
(Our work) CMB+BAOtr+PantheonPlus
(Our work) CMB+BAOtr
(Our work) CMB
(Akarsu et al., 2022) CMB+Pantheon+BAO+M_B
(Akarsu et al., 2022) CMB+Pantheon+Ly-α+M_B
(Akarsu et al., 2022) CMB+Pantheon+M_B
(Akarsu et al., 2022) CMB+Pantheon+BAO
(Akarsu et al., 2022) CMB+Pantheon+Ly-α
(Akarsu et al., 2022) CMB+Pantheon
(Akarsu et al., 2021) CMB+BAO
Λ_sCDM
ΛCDM
69.83 ± 0.37
73.16 ± 0.64
69.57 ± 0.42
72.82 ± 0.65
68.55 ± 0.44
$71.72^{+0.73}_{-0.92}$
68.84 ± 0.48
$73.3^{+1.2}_{-1.0}$
67.39 ± 0.55
$70.77^{+0.79}_{-2.7}$
68.29 ± 0.39
$69.48^{+0.48}_{-0.55}$
68.19 ± 0.38
72.0 ± 1.1
68.31 ± 0.52
$72.38^{+0.98}_{-1.10}$
$67.69^{+0.38}_{-0.43}$
$68.74^{+0.49}_{-0.55}$
67.68 ± 0.40
$70.17^{+0.96}_{-1.10}$
67.55 ± 0.53
$69.68^{+0.77}_{-1.40}$
67.81 ± 0.44
68.82 ± 0.55
Planck-ΛCDM
(67.36 ± 0.54)
SH0ES
(73.04 ± 1.04)
66 67 68 69 70 71 72 73 74 75
H_0 [km s^{-1}Mpc^{-1}]
H_0
80
70
M_B
−19.25
−19.35
1.5 2.5
$z_\dagger$
Λ_sCDM: Planck+BAOtr+PP&SH0ES+KiDS-1000
Λ_sCDM: Planck+BAOtr+PP&SH0ES
Λ_sCDM: Planck+BAOtr+PP
Λ_sCDM: Planck+BAOtr
Λ_sCDM: Planck

Data set	Planck	Planck+BAOtr	Planck+BAOtr +PP	Planck+BAOtr +PP&SH0ES	Planck+BAOtr +PP&SH0ES+KiDS-1000
Model	Λ_sCDM ΛCDM	Λ_sCDM ΛCDM	Λ_sCDM ΛCDM	Λ_sCDM ΛCDM	Λ_sCDM ΛCDM
$z_\dagger$	unconstrained $--$	$1.70^{+0.09}_{-0.19}(1.65)$ $--$	$1.87^{+0.13}_{-0.21}(1.75)$ $--$	$1.70^{+0.10}_{-0.13}(1.67)$ $--$	$1.72^{+0.09}_{-0.12}(1.70)$ $--$
M_B[mag]	$--$ $--$	$--$ $--$	$-19.317^{+0.021}_{-0.025}(-19.311)$ $-19.407 \pm 0.013(-19.411)$	$-19.290 \pm 0.017(-19.278)$ $-19.379 \pm 0.012(-19.373)$	$-19.282 \pm 0.017(-19.280)$ $-19.372 \pm 0.011(-19.369)$
H_0[km/s/Mpc]	$70.77^{+0.79}_{-2.70}(71.22)$ $67.39 \pm 0.55(67.28)$	$73.30^{+1.20}_{-1.00}(73.59)$ $68.84 \pm 0.48(68.61)$	$71.72^{+0.73}_{-0.92}(71.97)$ $68.55 \pm 0.44(68.54)$	$72.82 \pm 0.65(73.20)$ $69.57 \pm 0.42(69.73)$	$73.16 \pm 0.64(73.36)$ $69.83 \pm 0.37(69.96)$
Ω_m	$0.2860^{+0.0230}_{-0.0099}(0.2796)$ $0.3151 \pm 0.0075(0.3163)$	$0.2643^{+0.0072}_{-0.0090}(0.2618)$ $0.2958 \pm 0.0061(0.2984)$	$0.2768^{+0.0072}_{-0.0063}(0.2759)$ $0.2995 \pm 0.0056(0.2992)$	$0.2683 \pm 0.0052(0.2646)$ $0.2869 \pm 0.0051(0.2849)$	$0.2646 \pm 0.0052(0.2622)$ $0.2837 \pm 0.0045(0.2816)$
S_8	$0.801^{+0.026}_{-0.016}(0.791)$ $0.832 \pm 0.013(0.835)$	$0.777 \pm 0.011(0.772)$ $0.802 \pm 0.011(0.804)$	$0.791 \pm 0.011(0.794)$ $0.808 \pm 0.010(0.804)$	$0.783 \pm 0.010(0.777)$ $0.788 \pm 0.010(0.784)$	$0.774 \pm 0.009(0.773)$ $0.781 \pm 0.008(0.782)$
χ^2_{min}	2778.06 2780.52	2793.38 2820.30	4219.68 4235.18	4097.32 4138.26	4185.34 4226.50
$\ln\mathcal{B}_{ij}$	-1.28	-12.65	-7.52	-19.47	-19.77

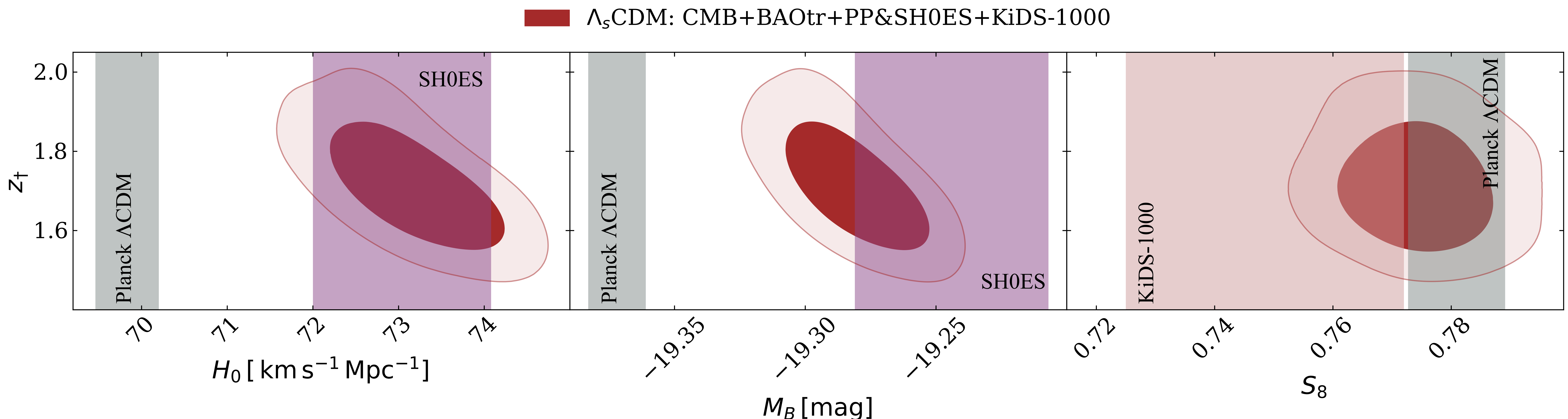

Data set	Planck	Planck+BAOtr	Planck+BAOtr +PP	Planck+BAOtr +PP&SH0ES	Planck+BAOtr +PP&SH0ES+KiDS-1000
Model	**Λ_sCDM**	**Λ_sCDM**	**Λ_sCDM**	**Λ_sCDM**	**Λ_sCDM**
	ΛCDM	**ΛCDM**	**ΛCDM**	**ΛCDM**	**ΛCDM**
$10^2\omega_b$	$2.241 \pm 0.015(2.252)$	$2.249 \pm 0.014(2.251)$	$2.245 \pm 0.014(2.247)$	$2.246 \pm 0.014(2.249)$	$2.250 \pm 0.013(2.252)$
	$2.238 \pm 0.014(2.235)$	$2.262 \pm 0.014(2.255)$	$2.256 \pm 0.013(2.248)$	$2.277 \pm 0.013(2.280)$	$2.282 \pm 0.013(2.283)$
ω_{cdm}	$0.1195 \pm 0.0012(0.1187)$	$0.1187 \pm 0.0012(0.1186)$	$0.1192 \pm 0.0011(0.1198)$	$0.1192^{+0.0010}_{-0.0012}(0.1186)$	$0.1184 \pm 0.0010(0.1180)$
	$0.1200 \pm 0.0012(0.1202)$	$0.1169 \pm 0.0010(0.1173)$	$0.1175 \pm 0.0010(0.1174)$	$0.1154 \pm 0.0009(0.1151)$	$0.1149 \pm 0.0008(0.1143)$
$100\theta_s$	$1.04189 \pm 0.00029(1.04207)$	$1.04199 \pm 0.00030(1.04194)$	$1.04196 \pm 0.00029(1.04181)$	$1.04197 \pm 0.00029(1.04167)$	$1.04199 \pm 0.00031(1.04168)$
	$1.04190^{+0.00027}_{-0.00031}(1.04178)$	$1.04218 \pm 0.00028(1.04211)$	$1.04213 \pm 0.00027(1.04225)$	$1.04236 \pm 0.00028(1.04242)$	$1.04242 \pm 0.00029(1.04218)$
$ln(10^{10}A_s)$	$3.040 \pm 0.014(3.046)$	$3.039 \pm 0.015(3.034)$	$3.042 \pm 0.014(3.044)$	$3.039 \pm 0.014(3.038)$	$3.037 \pm 0.014(3.045)$
	$3.046 \pm 0.014(3.049)$	$3.058^{+0.014}_{-0.017}(3.053)$	$3.056 \pm 0.016(3.047)$	$3.064^{+0.015}_{-0.017}(3.063)$	$3.062^{+0.013}_{-0.016}(3.079)$
n_s	$0.9669 \pm 0.0043(0.9664)$	$0.9695 \pm 0.0041(0.9692)$	$0.9679 \pm 0.0039(0.9644)$	$0.9682 \pm 0.0040(0.9711)$	$0.9695 \pm 0.0043(0.9701)$
	$0.9657 \pm 0.0041(0.9658)$	$0.9733 \pm 0.0039(0.9706)$	$0.9715 \pm 0.0035(0.9728)$	$0.9768 \pm 0.0038(0.9801)$	$0.9786 \pm 0.0035(0.9797)$
τ_{reio}	$0.0528 \pm 0.0073(0.0569)$	$0.0532 \pm 0.0077(0.0515)$	$0.0534 \pm 0.0073(0.0544)$	$0.0522 \pm 0.0073(0.0555)$	$0.0525 \pm 0.0074(0.0584)$
	$0.0550 \pm 0.0072(0.5488)$	$0.0639^{+0.0073}_{-0.0087}(0.0608)$	$0.0624^{+0.0074}_{-0.0086}(0.0586)$	$0.0684^{+0.0076}_{-0.0089}(0.0685)$	$0.0678^{+0.0067}_{-0.0085}(0.0771)$
$z_\dagger$	unconstrained	$1.70^{+0.09}_{-0.19}(1.65)$	$1.87^{+0.13}_{-0.21}(1.75)$	$1.70^{+0.10}_{-0.13}(1.67)$	$1.72^{+0.09}_{-0.12}(1.70)$
	$--$	$--$	$--$	$--$	$--$
$\chi^2_{\min}$	2778.06	2793.38	4219.68	4097.32	4185.34
	2780.52	2820.30	4235.18	4138.26	4226.50
$\ln\mathcal{Z}$	-1423.17	-1432.71	-2144.75	-2084.37	-2133.85
	-1424.45	-1445.36	-2152.27	-2103.84	-2153.62
$\ln\mathcal{B}_{ij}$	-1.28	-12.65	-7.52	-19.47	-19.77

Data set	Planck	Planck+BAOtr	Planck+BAOtr +PP	Planck+BAOtr +PP&SH0ES	Planck+BAOtr +PP&SH0ES+KiDS-1000
Model	Λ_sCDM ΛCDM	Λ_sCDM ΛCDM	Λ_sCDM ΛCDM	Λ_sCDM ΛCDM	Λ_sCDM ΛCDM
z_{reio}	$7.43^{+0.78}_{-0.67}(7.83)$ $7.75 \pm 0.72(7.76)$	$7.42 \pm 0.78(7.25)$ $8.52 \pm 0.76(8.25)$	$7.47 \pm 0.74(7.59)$ $8.39 \pm 0.76(8.05)$	$7.34 \pm 0.76(7.67)$ $8.87 \pm 0.75(8.88)$	$7.34 \pm 0.74(7.94)$ $8.79^{+0.64}_{-0.75}(9.64)$
Y_P	$0.247856 \pm 0.000063(0.247905)$ $0.247842 \pm 0.000062(0.247832)$	$0.247889 \pm 0.000060(0.247901)$ $0.247944 \pm 0.000059(0.247914)$	$0.247876 \pm 0.000058(0.247881)$ $0.247921^{+0.000059}_{-0.000053}(0.247888)$	$0.247877 \pm 0.000061(0.247887)$ $0.248010 \pm 0.000056(0.248020)$	$0.247895 \pm 0.000057(0.247903)$ $0.248031 \pm 0.000055(0.248034)$
z_d	$1060.03 \pm 0.29(1060.22)$ $1059.99 \pm 0.28(1059.95)$	$1060.15 \pm 0.29(1060.22)$ $1060.28 \pm 0.28(1060.16)$	$1060.12 \pm 0.29(1060.19)$ $1060.21 \pm 0.27(1060.03)$	$1060.12 \pm 0.30(1060.15)$ $1060.52 \pm 0.28(1060.55)$	$1060.15 \pm 0.27(1060.16)$ $1060.59 \pm 0.29(1060.56)$
r_d[Mpc]	$147.17 \pm 0.27(147.28)$ $147.07^{+0.24}_{-0.27}(147.06)$	$147.31 \pm 0.26(147.30)$ $147.65 \pm 0.25(147.63)$	$147.20 \pm 0.25(147.03)$ $147.55^{+0.24}_{-0.21}(147.65)$	$147.21 \pm 0.24(147.33)$ $147.87 \pm 0.23(147.93)$	$147.36 \pm 0.23(147.46)$ $147.96^{+0.25}_{-0.23}(148.10)$
t_0[Gyr]	$13.620^{+0.120}_{-0.042}(13.596)$ $13.793 \pm 0.023(13.800)$	$13.517^{+0.038}_{-0.049}(13.502)$ $13.745 \pm 0.021(13.756)$	$13.576^{+0.039}_{-0.034}(13.560)$ $13.755 \pm 0.020(13.760)$	$13.531 \pm 0.028(13.524)$ $13.716 \pm 0.020(13.710)$	$13.522 \pm 0.027(13.521)$ $13.706 \pm 0.018(13.709)$
M_B[mag]	−− −−	−− −−	$-19.317^{+0.021}_{-0.025}(-19.311)$ $-19.407 \pm 0.013(-19.411)$	$-19.290 \pm 0.017(-19.278)$ $-19.379 \pm 0.012(-19.373)$	$-19.282 \pm 0.017(-19.280)$ $-19.372 \pm 0.011(-19.369)$
H_0[km/s/Mpc]	$70.77^{+0.79}_{-2.70}(71.22)$ $67.39 \pm 0.55(67.28)$	$73.30^{+1.20}_{-1.00}(73.59)$ $68.84 \pm 0.48(68.61)$	$71.72^{+0.73}_{-0.92}(71.97)$ $68.55 \pm 0.44(68.54)$	$72.82 \pm 0.65(73.20)$ $69.57 \pm 0.42(69.73)$	$73.16 \pm 0.64(73.36)$ $69.83 \pm 0.37(69.96)$
ω_m	$0.1426 \pm 0.0011(0.1418)$ $0.1431 \pm 0.0011(0.1432)$	$0.1418 \pm 0.0011(0.1418)$ $0.1401 \pm 0.0010(0.1405)$	$0.1423 \pm 0.0010(0.1429)$ $0.1407 \pm 0.0010(0.1406)$	$0.1422 \pm 0.0010(0.1418)$ $0.1388 \pm 0.0009(0.1385)$	$0.1416 \pm 0.0010(0.1411)$ $0.1384 \pm 0.0008(0.1378)$
Ω_m	$0.2860^{+0.0230}_{-0.0099}(0.2796)$ $0.3151 \pm 0.0075(0.3163)$	$0.2643^{+0.0072}_{-0.0090}(0.2618)$ $0.2958 \pm 0.0061(0.2984)$	$0.2768^{+0.0072}_{-0.0063}(0.2759)$ $0.2995 \pm 0.0056(0.2992)$	$0.2683 \pm 0.0052(0.2646)$ $0.2869 \pm 0.0051(0.2849)$	$0.2646 \pm 0.0052(0.2622)$ $0.2837 \pm 0.0045(0.2816)$
σ_8	$0.8210^{+0.0064}_{-0.0110}(0.8191)$ $0.8121^{+0.0055}_{-0.0061}(0.8136)$	$0.8278 \pm 0.0086(0.8260)$ $0.8076^{+0.0058}_{-0.0067}(0.8064)$	$0.8240 \pm 0.0074(0.8281)$ $0.8087 \pm 0.0062(0.8054)$	$0.8277 \pm 0.0075(0.8274)$ $0.8054 \pm 0.0064(0.8047)$	$0.8244 \pm 0.0067(0.8264)$ $0.8030 \pm 0.0055(0.8076)$
S_8	$0.801^{+0.026}_{-0.016}(0.791)$ $0.832 \pm 0.013(0.835)$	$0.777 \pm 0.011(0.772)$ $0.802 \pm 0.011(0.804)$	$0.791 \pm 0.011(0.794)$ $0.808 \pm 0.010(0.804)$	$0.783 \pm 0.010(0.777)$ $0.788 \pm 0.010(0.784)$	$0.774 \pm 0.009(0.773)(0.773)$ $0.781 \pm 0.008(0.782)$
$D_H(2.33)/r_d$	$8.960^{+0.280}_{-0.380}(9.218)$ $8.615 \pm 0.013(8.614)$	$9.240^{+0.035}_{-0.025}(9.252)$ $8.648 \pm 0.011(8.643)$	$9.201^{+0.041}_{-0.017}(9.222)$ $8.641 \pm 0.010(8.639)$	$9.232 \pm 0.025(9.242)$ $8.664 \pm 0.008(8.667)$	$9.249 \pm 0.025(9.261)$ $8.670 \pm 0.008(8.675)$
χ^2_{min}	2778.06 2780.52	2793.38 2820.30	4219.68 4235.18	4097.32 4138.26	4185.34 4226.50
$\ln\mathcal{Z}$	−1423.17 −1424.45	−1432.71 −1445.36	−2144.75 −2152.27	−2084.37 −2103.84	−2133.85 −2153.62
$\ln\mathcal{B}_{ij}$	−1.28	−12.65	−7.52	−19.47	−19.77

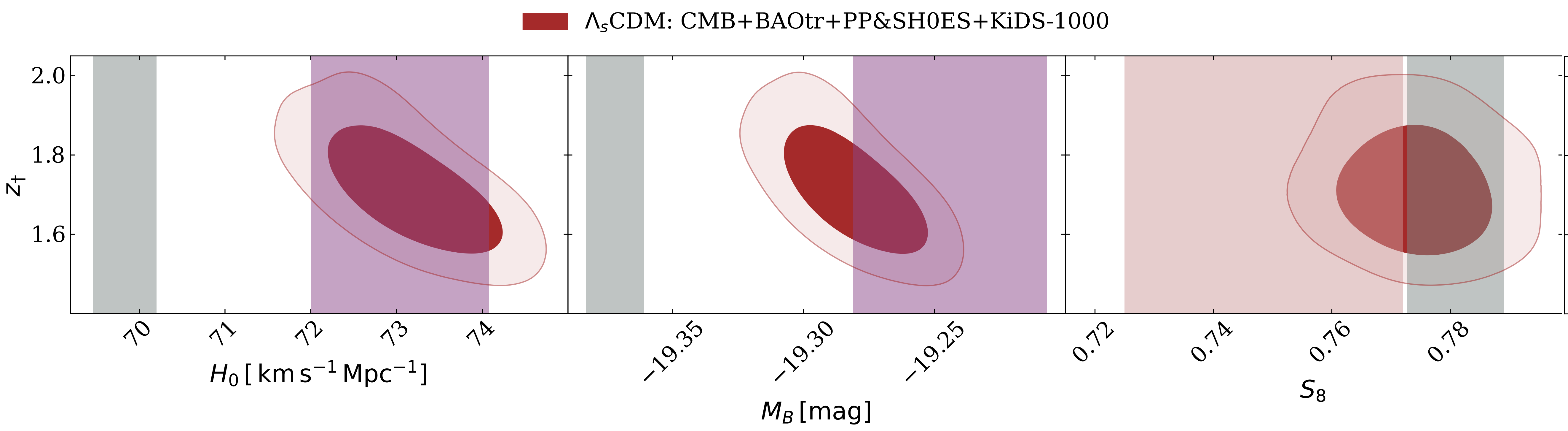

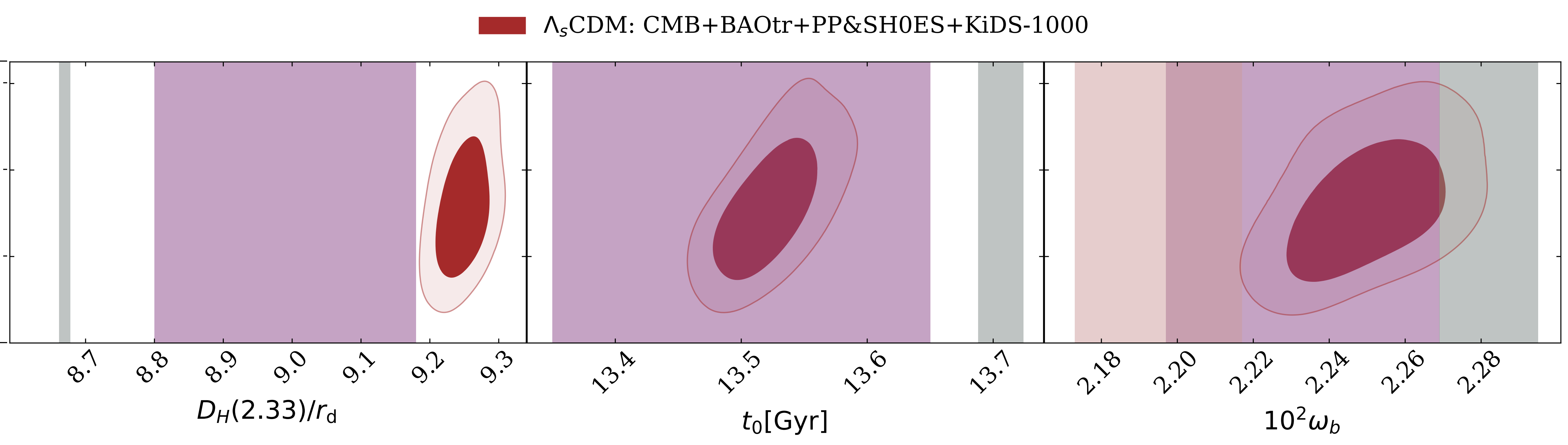

Data set	**Planck**	**Planck+BAOtr**	**Planck+BAOtr +PP**	**Planck+BAOtr +PP&SH0ES**	**Planck+BAOtr +PP&SH0ES+KiDS-1000**
Model	**Λ_sCDM**	**Λ_sCDM**	**Λ_sCDM**	**Λ_sCDM**	**Λ_sCDM**
	ΛCDM	**ΛCDM**	**ΛCDM**	**ΛCDM**	**ΛCDM**
$\boldsymbol{H_0}$	1.4σ	0.2σ	1.0σ	0.2σ	0.1σ
	4.8σ	3.7σ	4.3σ	3.1σ	2.9σ
$\boldsymbol{M_B}$	–	–	1.7σ	1.1σ	0.9σ
	–	–	4.5σ	3.5σ	3.3σ
$\boldsymbol{S_8}$	1.7σ	1.2σ	1.7σ	1.4σ	1.1σ
	3.1σ	2.0σ	2.3σ	1.5σ	1.3σ
$\boldsymbol{t_0}$	1.0σ	0.1σ	0.5σ	0.2σ	0.1σ
	1.9σ	1.6σ	1.7σ	1.4σ	1.4σ
$\boldsymbol{D_H(2.33)/r_d}$	0.2σ	1.3σ	1.1σ	1.3σ	1.4σ
	2.0σ	1.8σ	1.8σ	1.7σ	1.7σ
$\boldsymbol{\omega_b^{\mathrm{PCUV21}}}$	1.2σ	2.1σ	1.9σ	1.9σ	2.2σ
	1.6σ	2.6σ	2.4σ	3.1σ	3.4σ
$\boldsymbol{\omega_b^{\mathrm{LUNA}}}$	0.3σ	0.4σ	0.3σ	0.3σ	0.4σ
	0.1σ	0.8σ	0.6σ	1.1σ	1.3σ

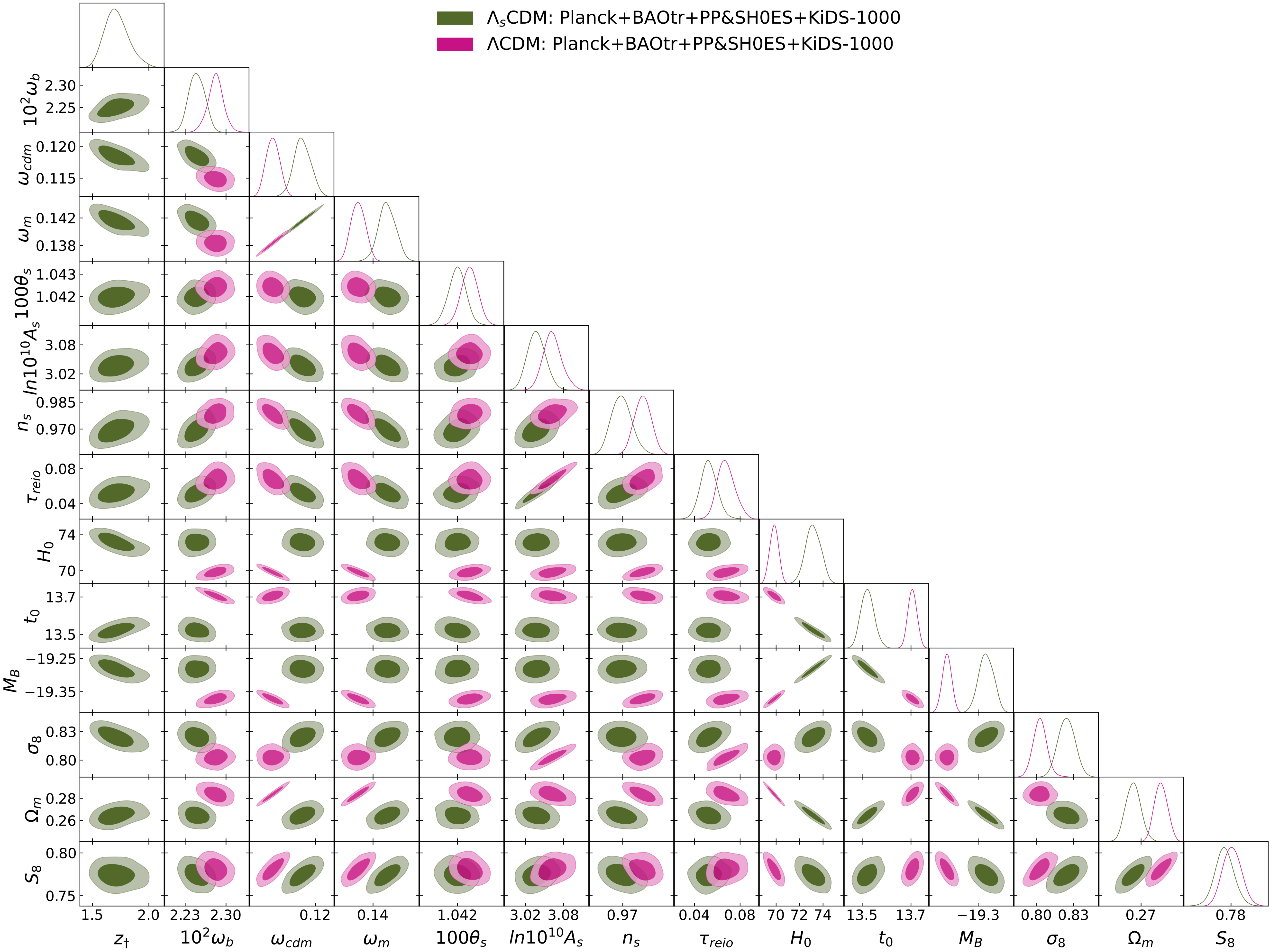

Λ_sCDM: Planck+BAOtr+PP&SH0ES+KiDS-1000
ΛCDM: Planck+BAOtr+PP&SH0ES+KiDS-1000
$z_\dagger$
$10^2\omega_b$
ω_{cdm}
ω_m
$100\theta_s$
$ln10^{10}A_s$
n_s
τ_{reio}
H_0
t_0
M_B
σ_8
Ω_m
S_8

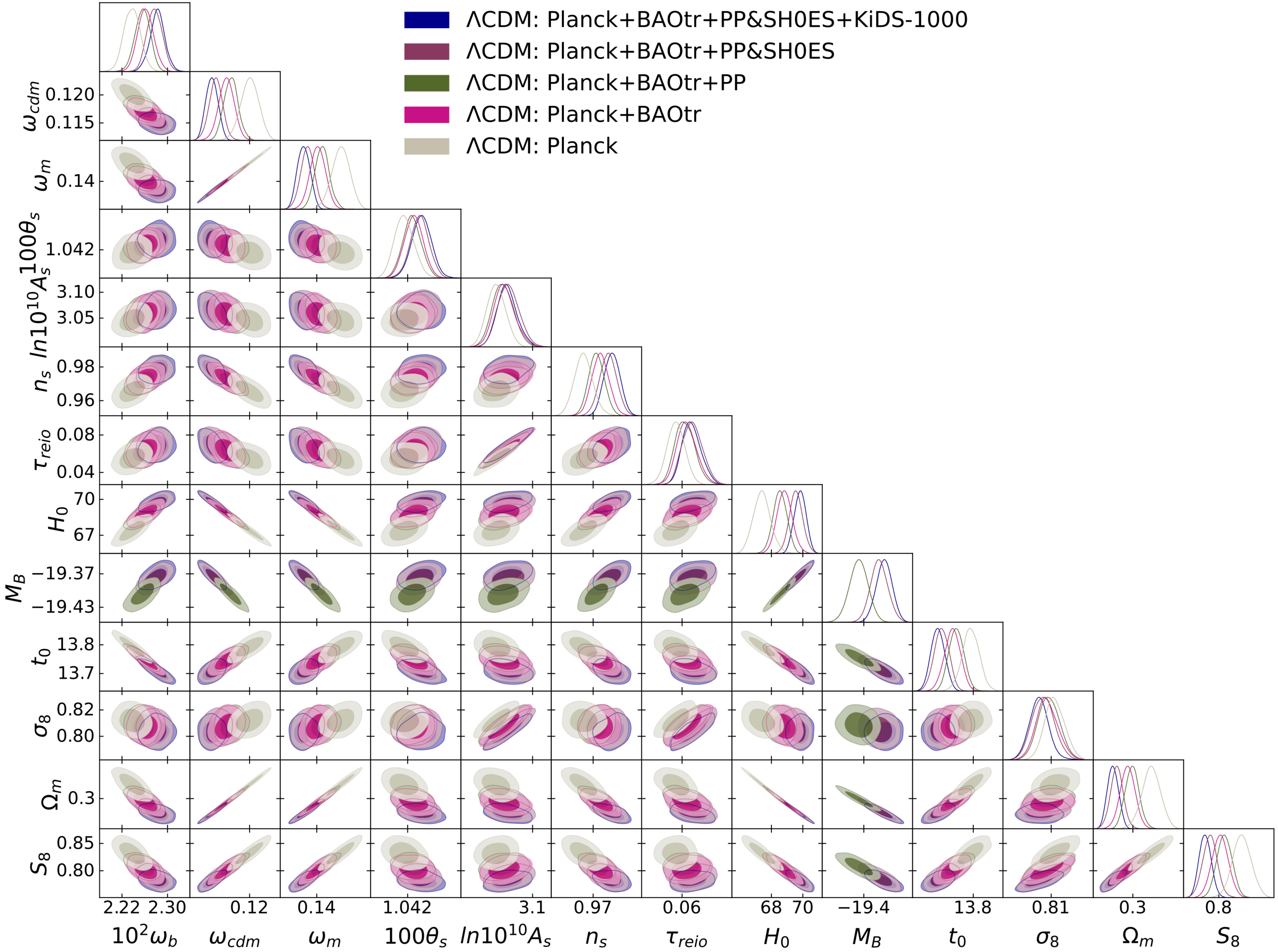
ΛCDM: Planck+BAOtr+PP&SH0ES+KiDS-1000
ΛCDM: Planck+BAOtr+PP&SH0ES
ΛCDM: Planck+BAOtr+PP
ΛCDM: Planck+BAOtr
ΛCDM: Planck
ω_{cdm}
ω_m
$100\theta_s$
$ln10^{10}A_s$
n_s
τ_{reio}
H_0
M_B
t_0
σ_8
Ω_m
S_8
$10^2\omega_b$

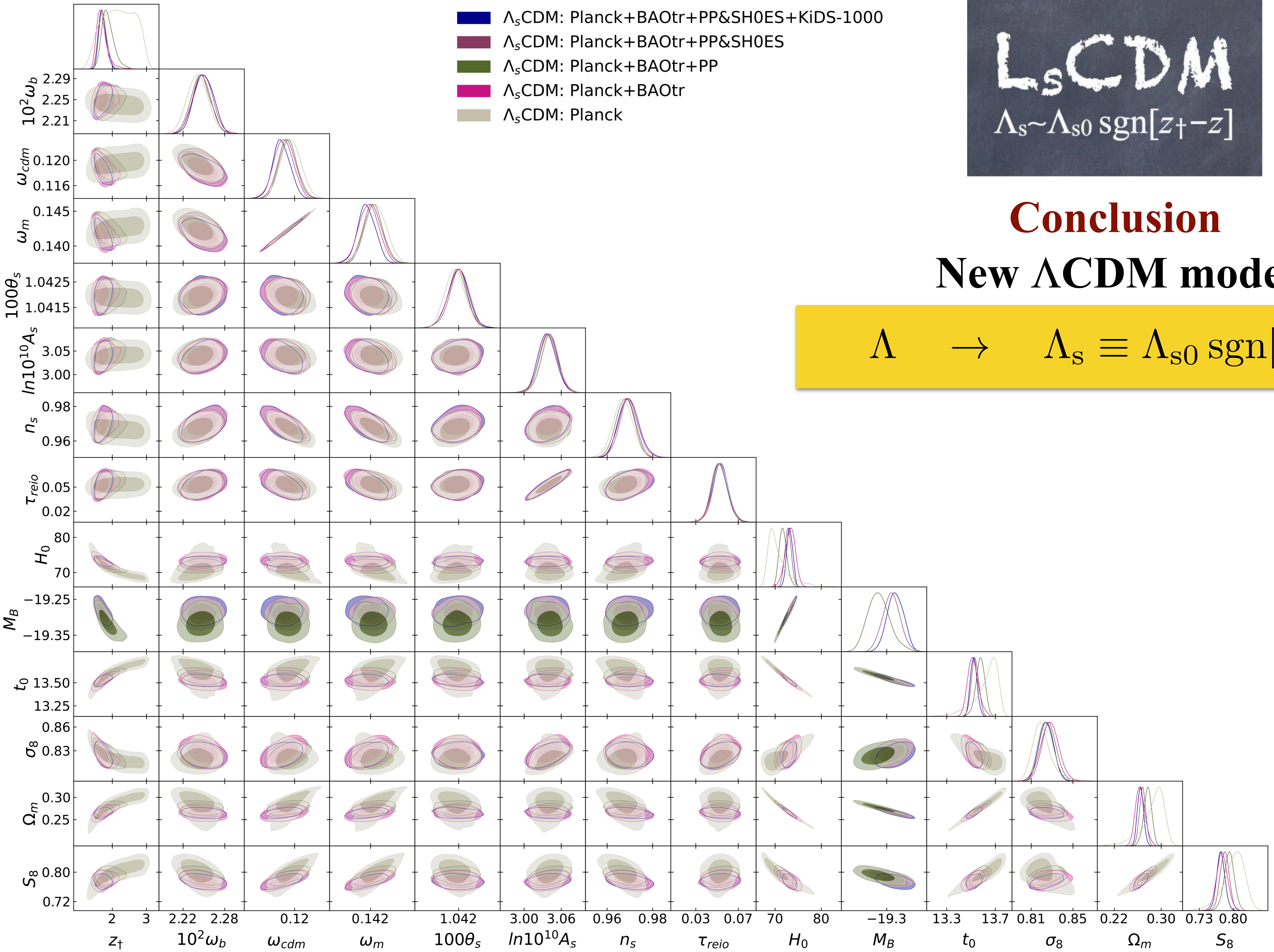

Conclusion

New ΛCDM model

$$\Lambda \quad \rightarrow \quad \Lambda_\mathrm{s} \equiv \Lambda_{\mathrm{s}0}\,\mathrm{sgn}[z_\dagger - z]$$

Ho'oleilana: An Individual Baryon Acoustic Oscillation?

R. Brent Tully,[1] Cullan Howlett,[2] and Daniel Pomarède[3]

[1] Institute for Astronomy, University of Hawaii, 2680 Woodlawn Drive, Honolulu, HI 96822, USA
[2] School of Mathematics and Physics, The University of Queensland, Brisbane, QLD 4072, Australia.
[3] Institut de Recherche sur les Lois Fondamentales de l'Univers, CEA Université Paris-Saclay, 91191 Gif-sur-Yvette, France

ABSTRACT

Theory of the physics of the early hot universe leads to a prediction of baryon acoustic oscillations that has received confirmation from the pair-wise separations of galaxies in samples of hundreds of thousands of objects. Evidence is presented here for the discovery of a remarkably strong *individual* contribution to the baryon acoustic oscillation (BAO) signal at $z = 0.068$, an entity that is given the name Ho'oleilana. The radius of the 3D structure is $155\, h_{75}^{-1}$ Mpc. At its core is the Boötes supercluster. The Sloan Great Wall, CfA Great Wall, and Hercules complex all lie within the BAO shell. The interpretation of Ho'oleilana as a BAO structure with our preferred analysis implies a value of the Hubble constant of $76.9^{+8.2}_{-4.8}$ km s^{-1} Mpc^{-1}.

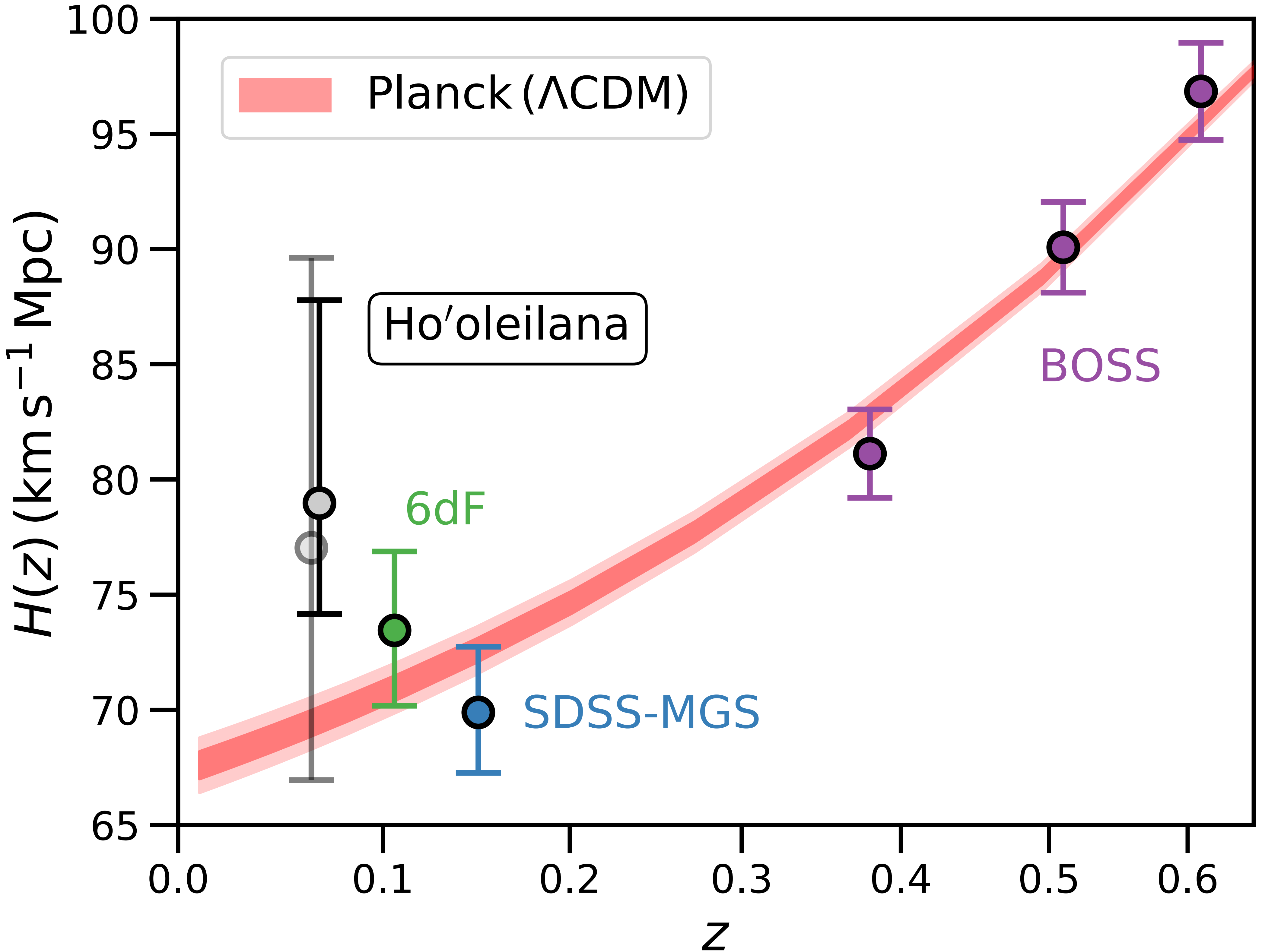

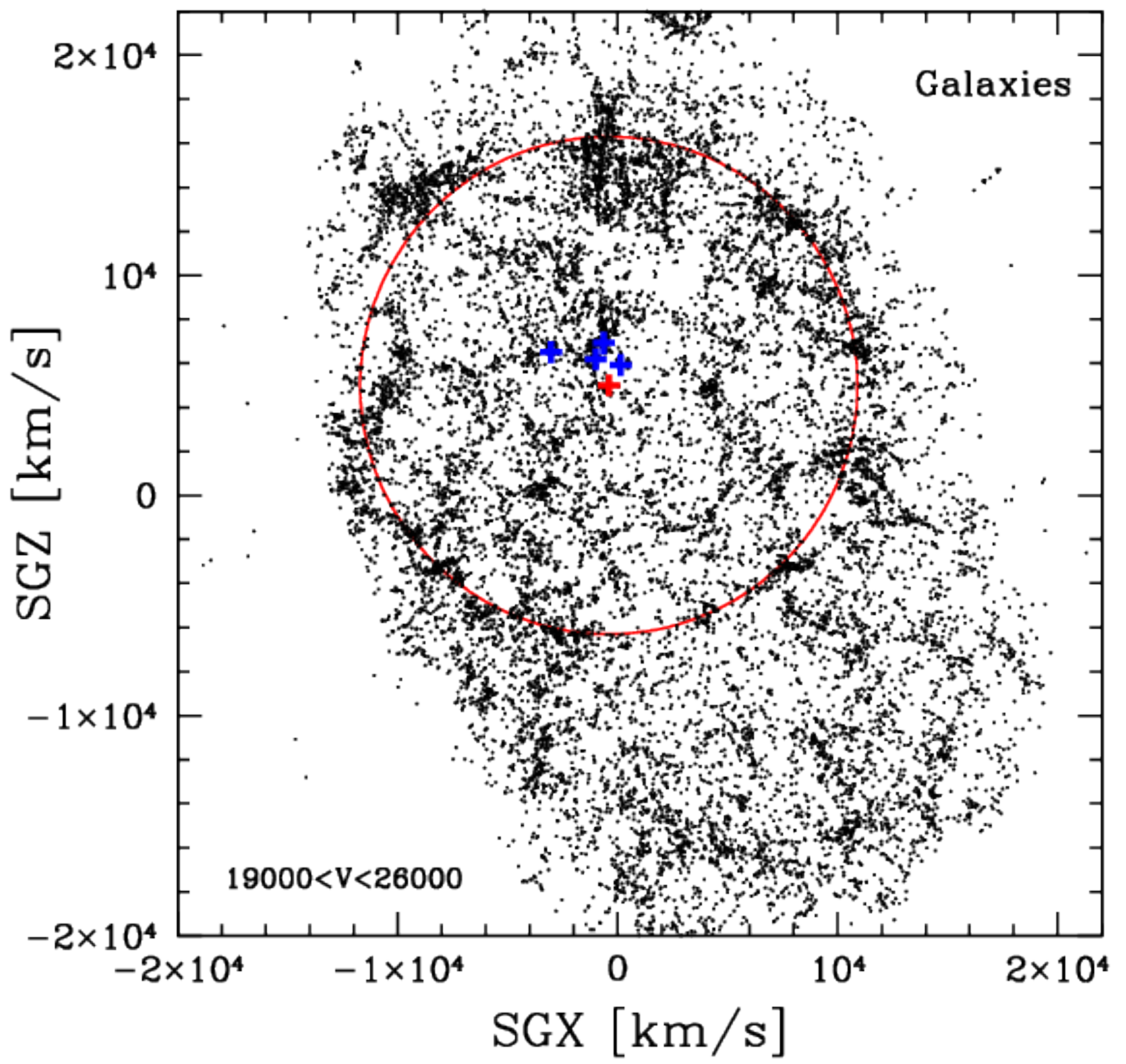

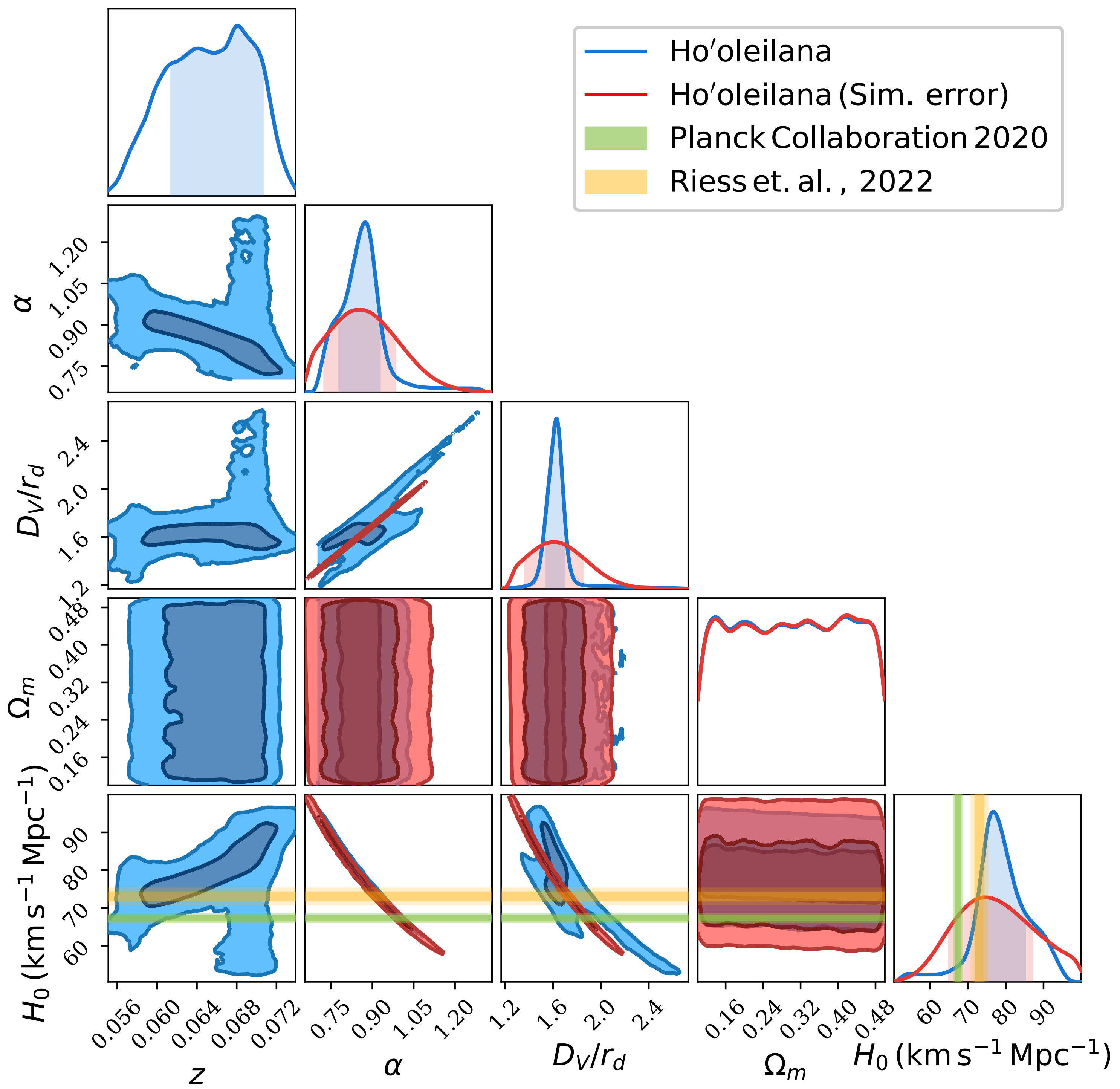

The growth of structure of the minimally interacting pressureless sources (baryons and CDM) after decoupling

$$\partial_t^2 \delta_{\rm m} = -2H\partial_t\delta_{\rm m} + 4\pi G\bar{\rho}_{\rm m}\delta_{\rm m}$$

arXiv:2307.12763

Dark energy in light of the early JWST observations: case for a negative cosmological constant?

Shahnawaz A. Adil,[a] Upala Mukhopadhyay,[b] Anjan A. Sen,[b] and Sunny Vagnozzi[c,d]

[a]Department of Physics, Jamia Millia Islamia, New Delhi-110025, India
[b]Centre for Theoretical Physics, Jamia Millia Islamia, New Delhi-110025, India
[c]Department of Physics, University of Trento, Via Sommarive 14, 38122 Povo (TN), Italy
[d]Trento Institute for Fundamental Physics and Applications (TIFPA)-INFN, Via Sommarive 14, 38122 Povo (TN), Italy

E-mail: shahnawaz188483@st.jmi.ac.in, rs.umukhopadhyay@jmi.ac.in, aasen@jmi.ac.in, sunny.vagnozzi@unitn.it

Abstract. Early data from the James Webb Space Telescope (JWST) has uncovered the existence of a surprisingly abundant population of very massive galaxies at extremely high redshift, which are hard to accommodate within the standard ΛCDM cosmology. We explore whether the JWST observations may be pointing towards more complex dynamics in the dark energy (DE) sector. Motivated by the ubiquity of anti-de Sitter vacua in string theory, we consider a string-inspired scenario where the DE sector consists of a negative cosmological constant (nCC) and a evolving component with positive energy density on top, whose equation of state is allowed to cross the phantom divide. We show that such a scenario can drastically alter the growth of structure compared to ΛCDM, and accommodate the otherwise puzzling JWST observations if the dynamical component evolves from the quintessence-like regime in the past to the phantom regime today: in particular, we demonstrate that the presence of a nCC (which requires a higher density for the evolving component) plays a crucial role in enhancing the predicted cumulative comoving stellar mass density. Our work reinforces the enormous potential held by observations of the abundance of high-z galaxies in probing cosmological models and new fundamental physics, including string-inspired ingredients.

arXiv:2308.07046

The density of virialized clusters as a probe of dark energy

Evangelos A. Paraskevas,[1] ⋆ Leandros Perivolaropoulos,[1] †
[1]*Department of Physics, University of Ioannina, GR-45110, Ioannina, Greece*

23 August 2023

ABSTRACT
We use the spherical collapse model to demonstrate that the observable average density of virialized clusters depends on the properties of dark energy along with the properties of gravity on cluster scales and can therefore be used as a probe of these properties. As an application of this approach we derive the predicted virialized densities and radii of cluster mass structures for a wide range of values of the cosmological constant (including negative values) as a function of the turnaround redshift. For the value of $\Omega_{\Lambda,0} = -0.7$ (with $\Omega_{m,0} = 0.3$) preferred by Λ sign-switching models (Λ_sCDM) proposed for the resolution of the Hubble and S_8 tensions, we find an amplification of the density of virialized clusters which can be as large as 80% compared to Planck18/ΛCDM for a turnaround redshift $z_{\rm max} \gtrsim 2$. Such an amplification may lead to more efficient early galaxy formation in this class of models in accordance with the recent findings of JWST.

Key words: Cosmology: Observations, Cosmology: Dark Energy